

Radiative corrections to the decay

$$H^+ \rightarrow W^+ A^0$$

A.G. Akeroyd^{a,*}, A. Arhrib^{b,c,†} and E. Naimi^{b,c}*a: KEK Theory Group, Tsukuba,
Ibaraki 305-0801, Japan**b: Département de Mathématiques, Faculté des Sciences et Techniques
B.P 416, Tanger, Morocco**c: UFR-High Energy Physics, Physics Departement, Faculty of Sciences
PO Box 1014, Rabat-Morocco***Abstract**

Full radiative corrections to the on-shell decay $H^+ \rightarrow W^+ A^0$ are computed in the framework of models with two Higgs doublets (THDM). Such a decay may be dominant for H^\pm over a wide range of parameter space relevant at present and future colliders. We show that the corrections may approach 50% and in particular are sensitive to λ_5 , which parametrizes the discrete symmetry breaking term. We suggest that a measurement of the branching ratio of $H^+ \rightarrow W^+ A^0$ may offer a possibility of measuring the magnitude of λ_5 .

PACS numbers:12.15.Lk,12.60.Fr

*E-mail: akeroyd@ccthmail.kek.jp

†E-mail: {arhrib,naimi}@fstt.ac.ma

1. Introduction

The phenomenology of charged Higgs bosons (H^\pm) has received much attention in recent years [1] since their discovery would provide conclusive evidence of physics beyond the Standard Model (SM) [2]. Charged Higgs bosons are predicted in many favourable extensions of the SM. The simplest model which contains a H^\pm is the Two Higgs Doublet Model (THDM), which is formed by adding an extra complex $SU(2)_L \otimes U(1)_Y$ scalar doublet to the SM lagrangian. Motivations for such a structure include CP-violation in the Higgs sector, supersymmetry, and a possible solution to the cosmological domain wall problem [3]. In particular, the Minimal Supersymmetric Standard Model (MSSM) [1] takes the form of a constrained THDM.

The phenomenology of H^\pm has received substantial attention at e^+e^- colliders [4],[5], hadron colliders [6], [7], [8], $\mu^+\mu^-$ colliders [9] and $\gamma\gamma$ colliders [10]. Most phenomenological studies have been carried out in the context of the MSSM. The combined null-searches from all four CERN LEP collaborations derive the lower limit $m_{H^\pm} \geq 77.3$ GeV (95% *c.l.*) [11], a limit which applies to all models in which $\text{BR}(H^\pm \rightarrow \tau\nu_\tau) + \text{BR}(H^\pm \rightarrow cs)=1$, where BR signifies branching ratio. Current mass bounds from LEP-II for the neutral pseudoscalar A^0 of the MSSM ($m_A \geq 75$ GeV) force $m_{H^\pm} \geq 109$ GeV in this model [12], which is stronger than the direct search limit above. Limits on m_{H^\pm} from the Fermilab Tevatron searches [13] are $\tan\beta$ dependent since a significant $\text{BR}(t \rightarrow H^+b)$ is required in order to obtain a visible signal. The limits are competitive with those from LEP-II for the regions $\tan\beta \leq 1$ or ≥ 40 .

In the MSSM, m_{H^\pm} and the mass of the pseudoscalar m_A are approximately degenerate for values greater than 200 GeV, and so the two body decay $H^\pm \rightarrow A^0W$ is never allowed for masses of interest at the CERN Large Hadron Collider (LHC). The three-body decay $H^\pm \rightarrow A^0W^* \rightarrow A^0 f\bar{f}$ is open for smaller m_{H^\pm} although it possesses a small branching ratio ($\text{BR} \leq 5\%$ for $m_{H^\pm} \geq 110$ GeV) [14]. Therefore for masses of interest at the LHC the principal decay channel is $H^\pm \rightarrow tb$, with decays to SUSY particles possibly open as m_{H^\pm} increases [15]. Recently there has been a surge of interest in studies of the MSSM with unconstrained CP-violating phases. In such scenarios $H^0 - A^0$ mixing may be induced radiatively [16] although this only leads to maximum mass splittings of the order 20 GeV for small values of $\tan\beta$; thus the two body decay would not be open even in this case.

Non-supersymmetric THDMs (hereafter to be called simply 'THDM') have also received considerable attention in the literature. In such models all the Higgs masses may be taken as free parameters (in contrast to the MSSM), thus allowing the possibility of the two body decay $H^\pm \rightarrow A^0W$ for certain choices of m_A and m_{H^\pm} . This decay mode possesses no mixing angle suppression, in contrast to $H^\pm \rightarrow h^0W$, and may compete with conventional decays. In fact, in a sizeable region of parameter space it may be the dominant channel. Even at LEP-II the three body decay $H^\pm \rightarrow A^0W^*$ may be dominant or even close to 100% in the THDM (Model I) [17] over a wide region of parameter space (see also Ref. [18]). Motivated by the results in Ref. [17] the authors calculated in Ref. [19] the Yukawa corrections to the decay $H^\pm \rightarrow A^0W^{(*)}$ and found that in the on-shell case the corrections may approach 50% for small values of $\tan\beta$. In this paper we complete that analysis and include the full bosonic corrections for the case of the W being on-shell.

Conventional Higgs searches at LEP-II assume the decays $H^\pm \rightarrow \tau\nu_\tau$ and cs [11], although the OPAL collaboration plans to include the $H^\pm \rightarrow A^0W^{(*)}$ topologies soon

[20]. In addition, the three-body decay may aid detection in the mass region $m_{H^\pm} \approx m_W$, which suffers from a sizeable background if H^\pm decays conventionally to two fermions. As we stressed in Ref. [19], the THDM with the popular Model II type structure is not expected to possess a H^\pm in the discovery range of LEP-II due to severe constraints on its mass ($m_{H^\pm} \geq 165$ GeV) derived from measurements of the rare decay $b \rightarrow s\gamma$ [21],[22]. In contrast, H^\pm in Model I avoids such constraints and so may be light. As mentioned above, it is precisely in Model I where the channel $H^\pm \rightarrow A^0 W^{(*)}$ can be dominant at LEP-II energies.

A recent study [23] showed that the decay $H^\pm \rightarrow A^0 W$ offers good chances of detection for H^\pm at the LHC, where an analysis in the context of the MSSM with an extra singlet superfield was carried out (NMSSM). Much of this work would be relevant for the THDM that we consider, although our bosonic corrections would not be directly applicable to the NMSSM, since the latter possesses two more neutral Higgs bosons in addition to different Higgs self-couplings.

The paper is organized as follows. In section 2 we introduce our notation and outline the form of the 1-loop corrections. In section 3 we explain the importance of including diagrams with the emission of a soft photon, $H^+ \rightarrow W^+ A^0 \gamma$, in order to keep the radiative corrections infra-red finite. Section 4 covers the various experimental and theoretical constraints that we impose. Section 5 presents our numerical results for the full corrections (bosonic and Yukawa), while section 6 contains our conclusions. The explicit form of the corrections is contained in the appendix.

2. Lowest order result and structure of one-loop radiative corrections

2.1 Lowest order result

We will be using the notation and conventions of our previous work [19], which we briefly review here. The momentum of the charged Higgs boson H^+ is denoted by p_H (p_H is incoming), p_W is the momentum of the W^+ gauge boson and p_A the momentum of the CP-odd A^0 (p_W and p_A are outgoing).

The relevant part of the lagrangian describing the interaction of the W^\pm with H^\pm and A^0 comes from the covariant derivative which is given by:

$$\mathcal{L} = \frac{e}{2s_W} W_\mu^+ (H^- \overleftrightarrow{\partial}^\mu A^0) + \text{h.c.} \quad (2.1)$$

This interaction is model independent (SUSY or non-SUSY) and depends only on standard parameters: electric charge (e) and Weinberg angle ($s_W = \sin \theta_W$).

The lowest-order Feynman diagram for the two-body decay $H^+ \rightarrow A^0 W^+$ is depicted in the following figure:

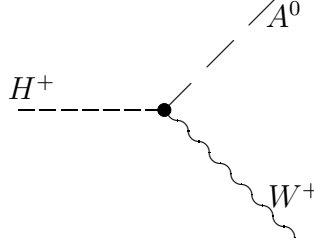


Figure. 1

In the Born approximation, the decay amplitude of the charged Higgs into an on-shell CP-odd Higgs boson A^0 and the gauge boson W^+ (Fig.1) can be written as:

$$\mathcal{M}^0(H^+ \rightarrow W^+ A^0) = \epsilon_\mu^* \Gamma_0^\mu \quad \text{where} \quad \Gamma_0^\mu = i \frac{e}{2s_W} (p_H + p_A)_\mu \quad (2.2)$$

Here ϵ_μ is the W^\pm polarization vector. We then have the following decay width:

$$\Gamma_{on}^0 = \frac{\alpha}{16s_W^2 m_W^2 m_{H^\pm}^3} \lambda^{\frac{3}{2}}(m_{H^\pm}^2, m_A^2, m_W^2) \quad (2.3)$$

where $\lambda = \lambda(x, y, z) = x^2 + y^2 + z^2 - 2(xy + xz + yz)$ is the familiar two-body phase space function. Note that in the MSSM the two-body decay of the charged Higgs boson into $W^+ A^0$ is kinematically not allowed. In this paper we will not present results for the case of W^\pm being off-shell. Ref. [19] evaluated the Yukawa corrections in the off-shell case for m_{H^\pm} in the range of LEP-II, finding maximum values of a few percent.

2.2 One-Loop radiative corrections

We shall evaluate the bosonic one-loop radiative corrections to the decay $H^+ \rightarrow W^+ A^0$, and add them to the Yukawa corrections previously evaluated in Ref. [19]. This set of corrections is ultra-violet (UV) and infra-red (IR) divergent. The UV singularities are treated by dimensional regularization [24] in the on-mass-shell renormalization scheme. The IR divergences are treated by the introduction of a small fictitious mass δ for the photon, which we shall explain in the next section.

The typical Feynman diagrams for the virtual corrections of order α are listed in figure 2. These contributions have to be supplemented by the counterterm renormalizing the vertex $H^+ A^0 W^-$ (eq 2.4). Note that in the THDM, the vertices $W^+ A^0 G^-$, $W^+ G^0 H^-$, $W^+ W^- A^0$ and $A^0 H^+ H^-$ are not present, and so the mixing $G^+ - H^+$, $G^0 - A^0$ and $W^+ - H^+$ does not give any contribution to our process. In our case, the gauge boson W is on-shell and so the mixing $W^\pm - G^\mp$ is absent. The full set of Feynman diagrams are generated and computed using the FeynArts and FeynCalc [25, 26] packages. The amplitudes of the typical vertices are given in terms of the one-loop scalar functions [27] and are written explicitly in appendix C. We also use the fortran FF-package [28] in the numerical analysis.

In what follows we will use the on-shell renormalization scheme developed in Ref. [19] (and refs therein). The vertex counterterm is given by:

$$\delta\mathcal{L} = \frac{e}{2s_W} W_\mu^+ (H^- \overleftrightarrow{\partial}^\mu A^0) \left(\frac{1}{2} \delta Z_{WW} + \frac{1}{2} \delta Z_{A^0 A^0} + \frac{1}{2} \delta Z_{H^\pm H^\pm} + \delta Z_e - \frac{\delta s_W}{s_W} \right) \quad (2.4)$$

where δZ_{WW} , $\delta Z_{A^0 A^0}$ and $\delta Z_{H^\pm H^\pm}$ are the wave function renormalization constants for the W^\pm gauge boson, A^0 and H^\pm Higgs boson defined as follows:

$$\delta Z_{ii} = -\frac{\partial \Sigma_{ii}(k^2)}{\partial k^2} \Big|_{k^2=m_i^2} \quad i = W, A^0, H^\pm \quad (2.5)$$

$$\delta m_i^2 = \text{Re} \Sigma_{ii}(m_i^2) \quad i = W, Z \quad (2.6)$$

where $\Sigma_{ii}(k^2)$ is the bare self-energy of the H^\pm , A^0 or W . The electric charge counterterm and $\frac{\delta s_W}{s_W}$ are defined as:

$$\frac{\delta s_W}{s_W} = -\frac{1}{2} \frac{c_W^2}{s_W^2} \left(\frac{\delta m_W^2}{m_W^2} - \frac{\delta m_Z^2}{m_Z^2} \right) \quad (2.7)$$

$$\delta Z_e = -\frac{1}{2} \delta Z_{\gamma\gamma} + \frac{1}{2} \frac{s_W}{c_W} \delta Z_{Z\gamma} = \frac{1}{2} \frac{\partial \Sigma_T^{\gamma\gamma}(k^2)}{\partial k^2} \Big|_{k^2=0} + \frac{s_W}{c_W} \frac{\Sigma_T^{Z\gamma}(0)}{m_Z^2} \quad (2.8)$$

The index T in $\Sigma_T^{\gamma\gamma}$ and $\Sigma_T^{Z\gamma}$ denotes that we take the transverse part. All the one-loop self-energies entering in the above equations (2.5–2.8) are given in appendix $D_1 \rightarrow D_6$.

The one-loop amplitude \mathcal{M}^1 (vertex plus counterterms) can be written as:

$$\mathcal{M}^1(H^+ \rightarrow W^+ A^0) = \frac{e}{2s_W} (\Gamma_H p_H^\mu + \Gamma_W p_W^\mu) \epsilon_\mu^* \quad (2.9)$$

where Γ_H and Γ_W can be cast as follow:

$$\Gamma_W = \Gamma_W^{\text{vertex}} + \delta \Gamma_W^{\text{vertex}} \quad (2.10)$$

$$\Gamma_H = \Gamma_H^{\text{vertex}} + \delta \Gamma_H^{\text{vertex}} \quad (2.11)$$

Here $\Gamma_{W,H}^{\text{vertex}}$ represents the vertex corrections and $\delta \Gamma_{W,H}^{\text{vertex}}$ is the counterterm contribution needed to remove the UV divergences contained in $\Gamma_{W,H}^{\text{vertex}}$.

The expressions of the counterterms are:

$$\begin{aligned} \delta \Gamma_W^{\text{vertex}} &= -(\delta Z_e - \frac{\delta s_W}{s_W} + \frac{1}{2}(\delta Z_{H^+ H^+} + \delta Z_{A^0} + \delta Z_W)) \\ \delta \Gamma_H^{\text{vertex}} &= -2\delta \Gamma_W^{\text{vertex}} \end{aligned} \quad (2.12)$$

In the on-shell case the interference term $2\text{Re} \mathcal{M}^{0*} \mathcal{M}^1$, found from squaring the one-loop corrected amplitude $|\mathcal{M}^0 + \mathcal{M}^1|^2$, is equal to $\Gamma_H |\mathcal{M}^0|^2$ [19]. Hence the one-loop corrected width Γ_{on}^1 can be written as

$$\Gamma_{on}^1 = (1 + \Gamma_H) \Gamma_{on}^0 \quad (2.13)$$

with Γ_H (defined by eq. 2.11) being interpreted as the fractional contribution to the tree-level width, Γ_{on}^0 . Note that Γ_W (eq. 2.10) does not contribute to Γ_{on}^1 .

3. Real photon emission: $H^+ \rightarrow W^+ A^0 \gamma$

The vertex correction supplemented by the counterterms is UV finite but there still remains infra-red divergences. These arise from the diagrams 2.10 and 2.11 with $V = \gamma$ and also from the wave function renormalisation constant $\delta Z_{H^\pm H^\pm}$ (Diagram 2.74) and

δZ_{WW} (diagrams 2.51, 2.52 and 2.53). In order to obtain a finite result, one has to add the correction from the emission of a real photon in the final state as drawn in figures 2.57 \rightarrow 2.60.

In terms of the momenta of the particles in the final state, the square amplitude of the process $H^+ \rightarrow A^0 W^+ \gamma$ is given by:

$$|M(H^+ \rightarrow A^0 W^+ \gamma)|^2 = -\frac{e^4}{s_W^2} \lambda(m_{H^\pm}^2, m_A^2, m_W^2) \left[\frac{m_{H^\pm}^2}{m_W^2} \frac{1}{(2p_H k_\gamma)^2} + \frac{1}{(2p_W k_\gamma)^2} + \left(\frac{m_A^2 - m_{H^\pm}^2}{m_W^2} - 1 \right) \frac{1}{(2p_W k_\gamma)(2p_H k_\gamma)} \right] \quad (3.1)$$

where k_γ denotes the momentum of the photon. Note that as a consequence of gauge invariance, the amplitude of the sum of the four diagrams (Figs. 2.57 \rightarrow 2.60), should vanish when multiplied by the four-momentum of the photon, which provides a good check of the calculation. The integrals over three body phase space can be found in [29], and one obtains the following expression:

$$\Gamma_{Br} = -\Gamma_{on}^0 \frac{e^2 M_{H^\pm}^2}{\pi^2 \lambda^{\frac{1}{2}}} \left[\frac{m_{H^\pm}^2}{m_W^2} I_{HH} + I_{WW} + \left(1 + \frac{m_{H^\pm}^2 - m_A^2}{m_W^2} \right) I_{HW} \right] \quad (3.2)$$

Where I_{HH} , I_{WW} and I_{HW} are given as follows:

$$\begin{aligned} I_{HH} &= \frac{1}{4m_{H^\pm}^4} \left\{ \lambda^{\frac{1}{2}} \log\left(\frac{\lambda}{\delta m_{H^\pm} m_A m_W}\right) - \lambda^{\frac{1}{2}} - (m_W^2 - m_A^2) \log\left(\frac{\beta_1}{\beta_2}\right) - m_{H^\pm}^2 \log(\beta_0) \right\} \\ I_{WW} &= \frac{1}{4m_{H^\pm}^2 m_W^2} \left\{ \lambda^{\frac{1}{2}} \log\left(\frac{\lambda}{\delta m_{H^\pm} m_A m_W}\right) - \lambda^{\frac{1}{2}} - (m_{H^\pm}^2 - m_A^2) \log\left(\frac{\beta_0}{\beta_2}\right) - m_W^2 \log(\beta_1) \right\} \\ I_{HW} &= \frac{1}{4m_{H^\pm}^4} \left\{ 2 \log\left(\frac{\lambda}{\delta m_{H^\pm} m_A m_W}\right) \log(\beta_2) + 2 \log^2(\beta_2) - \log^2(\beta_0) - \log^2(\beta_1) \right. \\ &\quad \left. + 2 \text{Sp}(1 - \beta_2^2) - \text{Sp}(1 - \beta_0^2) - \text{Sp}(1 - \beta_1^2) \right\} \end{aligned} \quad (3.3)$$

where $\lambda = \lambda(m_{H^\pm}^2, m_A^2, m_W^2)$ is the two body phase space, δ is a small fictious photon mass, Sp is the dilogarithm function and β_i are defined as:

$$\begin{aligned} \beta_0 &= \frac{m_{H^\pm}^2 - m_W^2 - m_A^2 + \lambda^{\frac{1}{2}}}{2m_W m_A}, & \beta_1 &= \frac{m_{H^\pm}^2 - m_W^2 + m_A^2 - \lambda^{\frac{1}{2}}}{2m_{H^\pm} m_A}, \\ \beta_2 &= \frac{m_{H^\pm}^2 + m_W^2 - m_A^2 - \lambda^{\frac{1}{2}}}{2m_{H^\pm} m_W} \end{aligned} \quad (3.4)$$

We stress here that the IR divergence contained in I_{HH} (I_{WW}) is cancelled by the wave function renormalisation constant of the charged Higgs H^\pm (W^\pm), while the IR divergence contained in I_{HW} is cancelled by the vertex diagrams 2.10 and 2.11 (with $V = \gamma$). One can confirm easily that adding the virtual corrections with the Bremsstrahlung diagrams yields an IR finite result. This feature has been checked both algebraically and numerically.

4. THDM scalar potential: Theoretical and Experimental constraints

In this section we define the THDM scalar potential that we will be using. In appendix A we list the trilinear and quartic scalar self-couplings which are relevant to our study. Other

relevant couplings involving Higgs boson interactions with gauge bosons and fermions can be found in Ref. [1]. For a full list of scalar trilinear and quartic couplings see Ref. [30]. It has been shown [1] that the most general THDM scalar potential which is both $SU(2)_L \otimes U(1)_Y$ and CP invariant is given by:

$$V(\Phi_1, \Phi_2) = \lambda_1(|\Phi_1|^2 - v_1^2)^2 + \lambda_2(|\Phi_2|^2 - v_2^2)^2 + \lambda_3((|\Phi_1|^2 - v_1^2) + (|\Phi_2|^2 - v_2^2))^2 + \lambda_4(|\Phi_1|^2|\Phi_2|^2 - |\Phi_1^\dagger\Phi_2|^2) + \lambda_5(Re(\Phi_1^\dagger\Phi_2) - v_1v_2)^2 + \lambda_6[Im(\Phi_1^\dagger\Phi_2)]^2 \quad (4.1)$$

where Φ_1 and Φ_2 have weak hypercharge $Y=1$, v_1 and v_2 are respectively the vacuum expectation values of Φ_1 and Φ_2 and the λ_i are real-valued parameters. Note that this potential violates the discrete symmetry $\Phi_i \rightarrow -\Phi_i$ softly by the dimension two term $\lambda_5 Re(\Phi_1^\dagger\Phi_2)$ and has the same general structure as the scalar potential of the MSSM. One can prove easily that for $\lambda_5 = 0$ the exact symmetry $\Phi_i \rightarrow -\Phi_i$ is recovered. We note that Ref. [31] lists the complete Higgs trilinear and quartic interactions for two 6 parameter potentials, referred to as 'Potential A' and 'Potential B'. Potential A is equivalent to our potential if $\lambda_5 \rightarrow 0$, and in this limit the feynman rules in the appendix A are in agreement with those in Ref. [31].

After electroweak symmetry breaking, the W and Z gauge bosons acquire masses given by $m_W^2 = \frac{1}{2}g^2v^2$ and $m_Z^2 = \frac{1}{2}(g^2 + g'^2)v^2$, where g and g' are the $SU(2)_L$ and $U(1)_Y$ gauge couplings and $v^2 = v_1^2 + v_2^2$. The combination $v_1^2 + v_2^2$ is thus fixed by the electroweak scale through $v_1^2 + v_2^2 = (2\sqrt{2}G_F)^{-1}$, and we are left with 7 free parameters in eq.(4.1), namely the $(\lambda_i)_{i=1,\dots,6}$ and $\tan\beta = v_2/v_1$. Meanwhile, three of the eight degrees of freedom of the two Higgs doublets correspond to the 3 goldstone bosons (G^\pm, G^0) and the remaining five become physical Higgs bosons: H^0, h^0 (CP-even), A^0 (CP-odd) and H^\pm . Their masses are obtained as usual by the shift $\Phi_i \rightarrow \Phi_i + v_i$ and read [1]:

$$m_A^2 = \lambda_6 v^2 \quad , \quad m_{H^\pm}^2 = \lambda_4 v^2 \quad , \quad m_{H,h}^2 = \frac{1}{2}[A + C \pm \sqrt{(A - C)^2 + 4B^2}]$$

where

$$A = 4v_1^2(\lambda_1 + \lambda_3) + v_2^2\lambda_5 \quad , \quad B = v_1v_2(4\lambda_3 + \lambda_5) \quad \text{and} \quad C = 4v_2^2(\lambda_2 + \lambda_3) + v_1^2\lambda_5 \quad (4.2)$$

The angle β diagonalizes both the CP-odd and charged scalar mass matrices, leading to the physical states H^\pm and A^0 . The CP-even mass matrix is diagonalized by the angle α , leading to the physical states H^0, h^0 , with α given by:

$$\sin 2\alpha = \frac{2B}{\sqrt{(A - C)^2 + 4B^2}} \quad , \quad \cos 2\alpha = \frac{A - C}{\sqrt{(A - C)^2 + 4B^2}} \quad (4.3)$$

It is then straightforward algebra to invert the previous equations to obtain the λ_i in terms of physical scalar masses, $\tan\beta$, α and λ_5 :

$$\lambda_4 = \frac{g^2}{2m_W^2}m_{H^\pm}^2 \quad , \quad \lambda_6 = \frac{g^2}{2m_W^2}m_A^2 \quad , \quad \lambda_3 = \frac{g^2}{8m_W^2} \frac{s_\alpha c_\alpha}{s_\beta c_\beta} (m_H^2 - m_h^2) - \frac{\lambda_5}{4} \quad (4.4)$$

$$\lambda_1 = \frac{g^2}{8c_\beta^2 m_W^2} [c_\alpha^2 m_H^2 + s_\alpha^2 m_h^2 - \frac{s_\alpha c_\alpha}{\tan\beta} (m_H^2 - m_h^2)] - \frac{\lambda_5}{4} (-1 + \tan^2\beta) \quad (4.5)$$

$$\lambda_2 = \frac{g^2}{8s_\beta^2 m_W^2} [s_\alpha^2 m_H^2 + c_\alpha^2 m_h^2 - s_\alpha c_\alpha \tan\beta (m_H^2 - m_h^2)] - \frac{\lambda_5}{4} (-1 + \frac{1}{\tan^2\beta}) \quad (4.6)$$

We are free to take as 7 independent parameters $(\lambda_i)_{i=1,\dots,6}$ and $\tan\beta$ or equivalently the four scalar masses, $\tan\beta$, α and one of the λ_i . In what follows we will take λ_5 as a free parameter.

In our analysis we will take into account the following constraints when the independent parameters are varied.

- The contributions to the $\delta\rho$ parameter from the Higgs scalars [32] should not exceed the current limits from precision measurements [33]: $-0.0017 \leq \delta\rho \leq 0.0027$.
- From the requirement of perturbativity for the top and bottom Yukawa couplings [34], $\tan\beta$ is constrained to lie in the range $0.3 \leq \tan\beta \leq 130$. Upper and lower bounds have also been obtained from the experimental limits on the processes $e^+e^- \rightarrow Z^* \rightarrow h^0\gamma$ and/or $e^+e^- \rightarrow A^0\gamma$. For very light h or A^0 (≈ 10 GeV) Ref. [35] derived $0.15 \leq \tan\beta \leq 75$, with the limits weakening for heavier $m_h(m_A)$. For our study we will restrict the discussion to values $\tan\beta \geq 0.5$.
- We require that tree-level unitarity is not violated in a variety of Higgs scattering processes.

We note here that tree-level unitarity constraints for the THDM scalar potential subjected to the exact symmetry $\Phi_i \rightarrow -\Phi_i$ were studied in Ref. [36]. To our knowledge such unitarity constraints have not been considered for the THDM scalar potential with the discrete symmetry $\Phi_i \rightarrow -\Phi_i$ softly violated by dimension two terms. A full study will be considered in future paper [37].

At high energy ($\sqrt{s} \gg m_H, m_h$) the requirement that the tree-level unitarity of the scattering matrix is preserved leads to the following constraint for the quartic scalar couplings:

$$|Q(S_1 S_2 \rightarrow S_1 S_2)| \leq 8\pi,$$

where Q represents the quartic coupling mediating the elastic scattering of scalars, $S_1 S_2 \rightarrow S_1 S_2$. Those diagrams contributing to the scattering process which are mediated by scalar trilinear couplings are heavily suppressed at high energies, resulting in only the quartic couplings being constrained. This in turn leads to restrictions on the allowed parameter space of Higgs masses and mixing angles. We will take into account the following scattering processes: $W_L^+ W_L^- \rightarrow W_L^+ W_L^-$, $Z_L Z_L \rightarrow Z_L Z_L$, $HH \rightarrow HH$, $hh \rightarrow hh$, $hH \rightarrow hH$, $hA \rightarrow hA$, $HA \rightarrow HA$, $AA \rightarrow AA$ and $H^+ H^- \rightarrow H^+ H^-$.

Note that the equivalence theorem relates the amplitude of longitudinal gauge boson $V = W^\pm, Z$ scattering to purely scalar scattering $S = G^\pm, G^0$. To a first approximation one finds: $\mathcal{M}(V_L^+ V_L^- \rightarrow V_L^+ V_L^-) \approx \mathcal{M}(SS \rightarrow SS) + \mathcal{O}(\frac{m_V}{\sqrt{s}})$ where \sqrt{s} is the centre of mass energy. Finally we are left with 9 quartic purely scalar couplings that are constrained by the requirement of unitarity.

5. Numerical results and discussion

In this section we present our numerical results for Γ_H , which is the fractional correction to the tree-level width (eq.2.13). We take the following experimental input for the physical parameters [38]. The fine structure constant: $\alpha = \frac{e^2}{4\pi} = 1/137.03598$, the gauge boson masses: $m_Z = 91.187$ GeV, $m_W = 80.41$ GeV, the input lepton masses: $m_e = 0.511$ MeV, $m_\mu = 0.1057$ GeV, $m_\tau = 1.784$ GeV. For the light quark masses we use the effective

values which are chosen in such a way that the experimentally extracted hadronic part of the vacuum polarizations is reproduced [39]: $m_d = 47 \text{ MeV}$, $m_u = 47 \text{ MeV}$, $m_s = 150 \text{ MeV}$, $m_c = 1.55 \text{ GeV}$, $m_b = 4.5 \text{ GeV}$. For the top quark mass we take $m_t = 175 \text{ GeV}$. In the on-shell scheme we consider, $\sin^2 \theta_W$ is given by $\sin^2 \theta_W \equiv 1 - \frac{m_W^2}{m_Z^2}$, and this expression is valid beyond tree-level.

Let us make some comment about the Yukawa corrections discussed in Ref. [19]. In the on-shell case, we showed that for small $\tan \beta$ in both Model I and II one can find large corrections of up to around 50%; in Model I for large $\tan \beta$ all fermion corrections decouple and reach a constant value of 3.3% for $\tan \beta > 4$, while Γ_H is enhanced in Model II for large $\tan \beta$. We stress at this stage that in the low $\tan \beta$ regime the corrections in Model I and Model II are practically identical. Since both perturbative constraints on the λ_i and unitarity constraints on the quartic scalar couplings are violated in the large $\tan \beta$ region we will only consider low values of $\tan \beta$ in our analysis. Thus our results are applicable to both Model I and II. Note that in order to satisfy the experimental constraint on $\delta\rho$ we have assumed (for the graphs we have plotted) that $\alpha = \beta - \frac{\pi}{2}$ and the charged Higgs boson mass m_{H^\pm} is quasi-degenerate with m_H .

In Fig.3 we plot Γ_H as a function of m_{H^\pm} for $m_H = m_{H^\pm} - 10 \text{ GeV}$, $m_h = 120 \text{ GeV}$, $m_A = 150 \text{ GeV}$ and $\alpha = \beta - \frac{\pi}{2}$ for several values of λ_5 . With the above set of parameters and for $\tan \beta = 0.5(1.5)$ and $\lambda_5 = 0$ in Fig.3.a (Fig.3.b), unitarity constraints on the quartic coupling require $m_{H^\pm} \leq 480(850) \text{ GeV}$, with this bound weakening for increasing λ_5 . In both Fig.3.a and Fig.3.b the Yukawa correction is positive and around 3.5% while the bosonic correction is negative. In Fig.3.a (with $\tan \beta = 0.5$) for small λ_5 , the bosonic correction is in the range $-0.6\% \rightarrow -8\%$ for $m_{H^\pm} \in [231, 710]$; for larger λ_5 it becomes strongly negative and dominates the Yukawa corrections. In Fig.3.b we take $\tan \beta = 1.5$ and this leads to important negative bosonic corrections in both the case of vanishing λ_5 and large λ_5 . For $\lambda_5 \approx 0$ (≈ 5) one can reach a correction of about -10% (-45%) for $m_{H^\pm} = 830 \text{ GeV}$.

Fig.4.a and Fig.4.b show the total contribution to Γ_H as function of m_A for $m_H = 504$, $m_h = 359$ and $m_{H^\pm} = 534 \text{ GeV}$. Fig.4.a corresponds to $\tan \beta = 0.8$ and Fig.4.b corresponds to $\tan \beta = 1.6$ (with $\alpha = \beta - \frac{\pi}{2}$). In both figures the Yukawa correction is positive in the region $m_A \leq 277 \text{ GeV}$ and $m_A \geq 352 \text{ GeV}$, while for $m_A \approx 350 \text{ GeV}$ the channel $A \rightarrow tt$ opens, leading to a very large negative correction. Note that the bosonic correction is negative for every value of m_A .

We can conclude that for the intermediate mass range of m_A and for $\lambda_5 \approx 0$ there is a cancellation between the Yukawa correction and the bosonic correction. For large λ_5 the contribution to Γ_H is dominated by the bosonic correction and is consequently negative. For $m_A \approx 350 \text{ GeV}$ ($\approx 2m_t$) there is constructive interference between the Yukawa and bosonic corrections.

In Fig.5 we plot the total contribution to Γ_H as a function of λ_5 for several values of $\tan \beta$. For $\tan \beta = 0.5, 1, 2$ the fermionic correction (independent of λ_5) takes the values -2.7%, 1.7%, 2.9%. One can easily see from the curves that Γ_H increases (and approaches -20%) when λ_5 is increased, which is expected from the form of the scalar coupling.

In Table 1 we present the bosonic (Γ_H^{bos}), top-bottom (Γ_H^{tb}) and total fermionic (Γ_H^{fer}) contributions to Γ_H for selected scalar sector parameters which respect both the experimental constraint on $\delta\rho$ and unitarity constraints. Γ_H^{fer} is the sum of Γ_H^{tb} and the light

fermion contributions, and $\Gamma_H = \Gamma_H^{bos} + \Gamma_H^{fer}$. It is clear from the table that there is cancellation between the top-bottom correction and the light fermionic corrections. The total fermionic correction is dominated by light fermions except for small $\tan\beta$ where top-bottom contributions can dominate. One can also see from the table the importance of the change of the sign of $\tan\alpha$.

It is clear that the parameter λ_5 plays an important role in the radiative corrections. The decay mode ($H^\pm \rightarrow A^0 W$) may in fact be dominant and in Fig.6 we show the ratio

$$R = \frac{\Gamma(H^\pm \rightarrow A^0 W)}{\Gamma(H^\pm \rightarrow A^0 W) + \Gamma(H^\pm \rightarrow tb)} \quad (5.1)$$

as a function of $\tan\beta$ for various values of m_{H^\pm} , fixing $m_A = 70$ GeV. We plot the tree-level width for ($H^\pm \rightarrow A^0 W$) given in Eq. 2.3, and the tree-level width for $H^\pm \rightarrow tb$ given in Ref. [14], assuming Model II type couplings. Since other channels such as $H^\pm \rightarrow h^0 W$ and $H^\pm \rightarrow H^0 W$ may be open the above ratio should be interpreted as the upper bound on $\text{BR}(H^\pm \rightarrow A^0 W)$. One can see that the decay $H^\pm \rightarrow A^0 W$ is always dominant for this choice of parameters, and clearly shows the importance of this channel. Given the possible large BR, an accurate measurement of $\text{BR}(H^\pm \rightarrow A^0 W)$ may allow one to obtain information on λ_5 . Other processes which are sensitive to λ_5 are $e^+e^- \rightarrow H^+H^-$ [5] and $H^\pm W^\mp$ [40], while theoretical bounds on the Higgs masses in the case of $\lambda_5 \neq 0$ are explored in Ref. [41].

m_{H^\pm}	m_H	m_h	m_A	λ_5	$\tan\beta$	$\tan\alpha$	Γ_H^{bos}	Γ_H^{tb}	Γ_H^{fer}	Γ_H
594.0	462.6	395.2	503.7	6.45	6.23	0.2	.38	-3.81	3.31	3.7
446.1	498.8	140.6	239.7	5.54	11.5	-0.74	-24.6	-3.81	3.31	-21
446.1	498.8	140.6	239.7	5.54	11.5	0.74	-2.53	-3.81	3.31	0.78
454.3	597.6	235.0	63.7	6.30	6.	-.90	-32.7	-3.83	3.28	-29.4
454.3	597.6	235.0	63.7	6.30	6.	0.90	0.26	-3.83	3.28	3.54
534.0	482.0	368.9	435.7	3.60	0.3	1.70	-0.51	0.17	7.3	6.79
534.0	482.0	399.8	442.3	2.20	1.9	0.80	0.36	-3.72	3.41	3.77
534.0	482.0	132.4	447.2	6.10	23.9	.50	7.7	-3.72	3.4	11.1
215.4	398.8	224.4	90.0	3.10	0.34	0.56	-1.02	-11.4	-4.35	-5.37
370.6	489.2	244.3	90.0	4.96	20.21	.94	-15.3	-4.2	2.8	-12.5
370.6	489.2	244.3	90.0	4.96	20.21	-0.94	-49.9	-4.2	2.8	-47.1
426.7	463.4	266.7	90.0	6.30	16.4	.40	0.72	-4.14	2.95	3.67

Table 1: Bosonic, top-bottom and fermionic corrections (as a percentage of tree-level width) for selected parameters. All masses are in GeV, and $\Gamma_H = \Gamma_H^{bos} + \Gamma_H^{fer}$.

6. Conclusions

We have computed the radiative corrections to the on-shell decay $H^+ \rightarrow A^0 W^+$ in the general Two Higgs Doublet Model, taking into account the experimental constraint on the ρ parameter and also unitarity constraints on the scalar sector parameters. We have included the Yukawa corrections, the full electroweak corrections (bosonic), and also the

real photon emission in the final state (Bremsstrahlung). The computation was done with dimensional regularization in the on-shell scheme. We find that the total radiative corrections may approach 50% in regions of parameter space for both small and large $\tan\beta$. The bosonic correction is sensitive to the soft discrete symmetry breaking parameter λ_5 , and may interfere both constructively and destructively with the Yukawa correction. For larger λ_5 the bosonic contribution becomes strongly negative and in general dominates the Yukawa correction. For $m_A \approx 2m_t$ and low $\tan\beta$ the Yukawa correction is maximized and interferes constructively with the bosonic correction, resulting in large negative corrections to the tree-level width. Finally, we showed that the decay $H^\pm \rightarrow A^0 W^\pm$ may supercede $H^\pm \rightarrow tb$ as the dominant decay channel, and thus a precise measurement of its branching ratio may allow information to be obtained on λ_5 .

Acknowledgements

A.G.A was supported by the Japan Society for Promotion of Science (JSPS). We thank C. Dove for reading the manuscript.

Appendix A: THDM trilinear and quartic scalar couplings

In this appendix we list the Feynman rules in the general THDM for the trilinear and quartic scalar couplings relevant for our study. All formulae are written in terms of the physical masses, α , β and the soft breaking term λ_5 . Note that in the trilinear couplings (quartic couplings) we have factorised out ie (ie^2). In the following $g_C = 1/(2s_W m_W s_{2\beta})$, $v^2 = \frac{2m_W^2}{g^2}$, $c_{\beta\alpha}^\pm = \cos(\beta \pm \alpha)$ and $s_{\beta\alpha}^\pm = \sin(\beta \pm \alpha)$.

A.1 Trilinear scalar coupling

$$g_{H^0 H^+ H^-} = -2g_c(m_{H^0}^2(c_\beta^3 s_\alpha + s_\beta^3 c_\alpha) + m_{H^\pm}^2 s_{2\beta} c_{\beta\alpha}^- - s_{\beta\alpha}^+ \lambda_5 v^2) \quad (\text{A.1})$$

$$g_{H^0 H^+ G^-} = g_c s_{2\beta} s_{\beta\alpha}^- (m_{H^0}^2 - m_{H^\pm}^2) \quad (\text{A.2})$$

$$g_{h^0 H^+ H^-} = -2g_c(m_{h^0}^2(c_\alpha c_\beta^3 - s_\alpha s_\beta^3) + m_{H^\pm}^2 s_{2\beta} s_{\beta\alpha}^- - c_{\beta\alpha}^+ \lambda_5 v^2) \quad (\text{A.3})$$

$$g_{h^0 H^+ G^-} = -g_c s_{2\beta} c_{\beta\alpha}^- (m_{h^0}^2 - m_{H^\pm}^2) \quad (\text{A.4})$$

$$g_{H^0 A^0 A^0} = -2g_c(m_{H^0}^2(s_\alpha c_\beta^3 + c_\alpha s_\beta^3) + m_A^2 s_{2\beta} c_{\beta\alpha}^- - s_{\beta\alpha}^+ \lambda_5 v^2) \quad (\text{A.5})$$

$$g_{H^0 A^0 G^0} = g_c s_{2\beta} s_{\beta\alpha}^- (m_{H^0}^2 - m_A^2) \quad (\text{A.6})$$

$$g_{h^0 A^0 A^0} = -2g_c(m_{h^0}^2(c_\alpha c_\beta^3 - s_\alpha s_\beta^3) + m_A^2 s_{2\beta} s_{\beta\alpha}^- - c_{\beta\alpha}^+ \lambda_5 v^2) \quad (\text{A.7})$$

$$g_{h^0 A^0 G^0} = g_c s_{2\beta} c_{\beta\alpha}^- (m_A^2 - m_{h^0}^2) \quad (\text{A.8})$$

$$g_{A^0 H^+ G^-} = i g_c s_{2\beta} (m_{H^\pm}^2 - m_A^2) \quad (\text{A.9})$$

A.2 Quartic scalar coupling

$$g_{H^0 H^0 H^0 H^0} = -12g_C^2 [m_{H^0}^2 (c_\beta s_\alpha^3 + s_\beta c_\alpha^3)^2 + m_{h^0}^2 s_\alpha^2 c_\alpha^2 s_{\beta\alpha}^-^2 - \lambda_5 v^2 (c_\alpha^2 - c_\beta^2)^2] \quad (\text{A.10})$$

$$g_{h^0 h^0 h^0 h^0} = -12g_C^2 [m_{H^0}^2 s_\alpha^2 c_\alpha^2 c_{\beta\alpha}^{-2} + m_{h^0}^2 (c_\beta c_\alpha^3 - s_\beta s_\alpha^3)^2 - \lambda_5 v^2 (c_\alpha^2 - s_\beta^2)^2] \quad (\text{A.11})$$

$$g_{A^0 A^0 A^0 A^0} = -12g_C^2 [m_{H^0}^2 (c_\alpha s_\beta^3 + s_\alpha c_\beta^3)^2 + m_{h^0}^2 (c_\alpha c_\beta^3 - s_\alpha s_\beta^3)^2 - \lambda_5 v^2 c_{2\beta}^2] \quad (\text{A.12})$$

$$g_{G^0 G^0 G^0 G^0} = -3g_C^2 s_{2\beta}^2 [m_{H^0}^2 c_{\beta\alpha}^{-2} + m_{h^0}^2 s_{\beta\alpha}^{-2}] \quad (\text{A.13})$$

$$g_{H^+ H^- H^+ H^-} = -8g_C^2 [m_{H^0}^2 (c_\alpha s_\beta^3 + s_\alpha c_\beta^3)^2 + m_{h^0}^2 (c_\alpha c_\beta^3 - s_\alpha s_\beta^3)^2 - \lambda_5 v^2 c_{2\beta}^2] \quad (\text{A.14})$$

$$g_{G^+ G^- G^+ G^-} = -2g_C^2 s_{2\beta}^2 [m_{H^0}^2 c_{\beta\alpha}^{-2} + m_{h^0}^2 s_{\beta\alpha}^{-2}] \quad (\text{A.15})$$

$$g_{H^0 H^0 h^0 h^0} = -4g_C^2 [m_{H^0}^2 s_\alpha c_\alpha (s_\beta c_\beta + 3s_\alpha c_\alpha s_{\beta\alpha}^{-2}) - m_{h^0}^2 s_\alpha c_\alpha (s_\beta c_\beta - 3s_\alpha c_\alpha c_{\beta\alpha}^{-2}) - \lambda_5 v^2 (3s_\alpha^2 c_\alpha^2 - s_\beta^2 c_\beta^2)] \quad (\text{A.16})$$

$$g_{H^0 H^0 A^0 A^0} = -2g_C^2 [2m_{H^0}^2 (s_\alpha c_\beta^3 + c_\alpha s_\beta^3) (c_\beta s_\alpha^3 + s_\beta c_\alpha^3) + 2m_{h^0}^2 s_\alpha c_\alpha s_{\beta\alpha}^{-2} (c_\alpha c_\beta^3 - s_\alpha s_\beta^3) + m_A^2 (c_\beta^2 - s_\beta^2) (c_\alpha^2 - s_\beta^2 + 2s_\alpha s_\beta c_{\beta\alpha}^{-2}) + 2\lambda_5 v^2 (c_{2\beta} (c_\alpha^2 s_\beta^4 - s_\alpha^2 c_\beta^4) - s_\beta^2 c_\alpha^2 (1 + s_{2\alpha} s_{2\beta}))] \quad (\text{A.17})$$

$$g_{h^0 h^0 A^0 A^0} = -2g_C^2 [2m_{H^0}^2 (s_\alpha c_\beta^3 + c_\alpha s_\beta^3) s_\alpha c_\alpha c_{\beta\alpha}^{-2} + 2m_{h^0}^2 (c_\beta c_\alpha^3 - s_\beta s_\alpha^3) (c_\alpha c_\beta^3 - s_\alpha s_\beta^3) + m_A^2 (c_\beta^2 - s_\beta^2) (s_\alpha^2 + s_\beta^2 - 2s_\alpha s_\beta c_{\beta\alpha}^{-2}) + 2\lambda_5 v^2 (c_{2\beta} (s_\alpha^2 s_\beta^4 - c_\alpha^2 c_\beta^4) - s_\beta^2 c_\alpha^2 (1 - s_{2\alpha} s_{2\beta}))] \quad (\text{A.18})$$

Appendix B: One-loop functions

Let us briefly recall the definitions of scalar and tensor integrals [27] we use. The inverse of the propagators are denoted by

$$d_0 = q^2 - m_0^2, \quad d_i = (q + p_i)^2 - m_i^2$$

where the p_i are the momenta of the external particles (always incoming).

B.1 One-point function:

$$A_0(m_0^2) = \frac{(2\pi\mu)^{(4-D)}}{i\pi^2} \int d^D q \frac{1}{d_0}$$

where μ is an arbitrary renormalization scale and D is the space-time dimension.

B.2 Two-point functions:

$$B_{0,\mu,\mu\nu} = \frac{(2\pi\mu)^{(4-D)}}{i\pi^2} \int d^D q \frac{\{1, q_\mu, q_\mu q_\nu\}}{d_0 d_1}$$

Using Lorentz covariance, one gets for the vector integral

$$B_\mu = p_{1\mu} B_1 \\ B_{\mu\nu} = g_{\mu\nu} B_{00} + p_{1\mu} p_{1\nu} B_{11}$$

with the scalar functions $\{B_1, B_{00}, B_{11}\}(p_1^2, m_0^2, m_1^2)$.

B.3 Three-point functions:

$$C_{0,\mu,\mu\nu} = \frac{(2\pi\mu)^{(4-D)}}{i\pi^2} \int d^D q \frac{\{1, q_\mu, q_\mu q_\nu\}}{d_0 d_1 d_2}$$

where $p_{ij}^2 = (p_i + p_j)^2$. Lorentz covariance yields the decomposition

$$C_\mu = p_{1\mu} C_1 + p_{2\mu} C_2 \quad (\text{B.1})$$

$$C_{\mu\nu} = g_{\mu\nu} C_{00} + p_{1\mu} p_{1\nu} C_{11} + p_{2\mu} p_{2\nu} C_{22} + (p_{1\mu} p_{2\nu} + p_{2\mu} p_{1\nu}) C_{12} \quad (\text{B.2})$$

with the scalar functions $C_{i,j}(p_1^2, p_{12}^2, p_2^2, m_0^2, m_1^2, m_2^2)$.

All the tensor coefficients can be algebraically reduced to the basic scalar integrals A_0 , B_0 and C_0 . The analytical expression of all the scalar functions can be found in [?, 28].

Appendix C: One-loop vertex: $H^+ \rightarrow WA^0$

In this appendix we will list the analytic expression for each generic diagram of Fig.2. The sum over all the particle contents yields the corresponding contribution to the one-loop amplitude for $H^+ \rightarrow WA^0$:

C. 1 Fermionic Loops

The diagram with the uud triangle, Fig.2.1, yields the following contribution to the one-loop amplitude:

$$\begin{aligned} M_{2.1} = & -\frac{e\alpha N_C}{2\sqrt{2}\pi s_W} Y_{uu} \{Y_{ud}^L (2B_0 + B_1) + m_u C_0 (m_u Y_{ud}^L + m_d Y_{ud}^R) \\ & + Y_{ud}^L [m_W^2 C_2 - 2C_{00} - 2m_A^2 C_{11} + C_{12} (m_{H^\pm}^2 - m_W^2 - m_A^2)]\} \end{aligned} \quad (\text{C.1})$$

$N_C = 3(1)$ for quarks (leptons). Therein, all the B_0 , B_1 , C_i and C_{ij} have the same arguments:

$$[B_0, B_1](m_{H^\pm}^2, m_u^2, m_d^2), [C_i, C_{ij}](m_A^2, m_{H^\pm}^2, p_W^2, m_u^2, m_d^2)$$

The summation has to be performed over all fermion families; in practice only the third quark generation is relevant.

The corresponding expression for the the diagram with the ddu triangle in Fig.2.2 is obtained from the previous one by making the following replacements:

$$Y_{ud}^L \longleftrightarrow Y_{ud}^R, \quad Y_{uu} \longleftrightarrow Y_{dd}, \quad m_u \longleftrightarrow m_d$$

C. 2 Bosonic Loops

Diagram 2.3

$$M_{2.3} = \frac{e\alpha}{2\pi} g_{H^+ S_i S_k} g_{A S_i S_j} g_{W^+ S_j S_k} C_1(m_A^2, m_{H^\pm}^2, m_W^2, m_{S_j}^2, m_{S_i}^2, m_{S_k}^2) \quad (\text{C.2})$$

The couplings are summarized in the following table:

(S_i, S_j, S_k)	$g_{H^+ S_i S_k}$	$g_{A S_i S_j}$	$g_{W^+ S_j S_k}$
(h, A, H^+)	$g_{hH^+H^+}$	g_{hAA}	$\frac{1}{2s_W}$
(G^+, H^+, h)	$g_{hH^+G^+}$	$g_{AG^+H^+}$	$\frac{c_{\beta\alpha}}{2s_W}$
(G^+, H^+, H)	$g_{HH^+G^+}$	$-ig_{AH^+G^+}$	$-\frac{s_{\beta\alpha}^-}{2s_W}$
(G^+, H^+, A)	$-ig_{AH^+G^+}$	$-ig_{AH^+G^+}$	$\frac{1}{2s_W}$
(H, A, H^+)	$g_{HH^+H^+}$	g_{HAA}	$\frac{1}{2s_W}$
(h, G^0, G^+)	$g_{hH^+G^+}$	g_{hAG^0}	$\frac{1}{2s_W}$
(H, G^0, G^+)	$g_{HH^+G^+}$	g_{HAG^0}	$\frac{1}{2s_W}$
(A, h, G^+)	$-ig_{AH^+G^+}$	g_{hAA}	$\frac{s_{\beta\alpha}^-}{2s_W}$
(A, H, G^+)	$-ig_{AH^+G^+}$	g_{HAA}	$\frac{c_{\beta\alpha}}{2s_W}$
(H^+, G^+, h)	$g_{hH^+H^+}$	$-ig_{AH^+G^+}$	$-\frac{s_{\beta\alpha}^-}{2s_W}$
(H^+, G^+, H)	$g_{HH^+H^+}$	$-ig_{AH^+G^+}$	$-\frac{c_{\beta\alpha}}{2s_W}$

Diagram 2.4

$$M_{2.4}[h] = -\frac{e\alpha c_{\beta\alpha}^{-2}}{16\pi s_W^3} \{ -4B_0(m_{H^\pm}^2, m_h^2, m_W^2) + [2(-m_A^2 + m_{H^\pm}^2 - 2m_Z^2) - 4p_W^2]C_0[h] \\ + [3(-m_A^2 + m_{H^\pm}^2) - 4p_W^2]C_1[h] + [4(-m_A^2 + m_{H^\pm}^2) - 4p_W^2]C_2[h] + 4C_{00}[h] \\ + [m_{H^\pm}^2 + 3m_A^2 - p_W^2]C_{11}[h] - 2[m_{H^\pm}^2 - m_A^2]C_{12}[h] \} \quad (\text{C.3})$$

$$M_{2.4}[H] = M_{2.4}[h][c_{\beta\alpha}^{-2} \rightarrow s_{\beta\alpha}^{-2}, m_h \rightarrow m_H, h \rightarrow H] \quad (\text{C.4})$$

Where the arguments of C_i and C_{ij} are given as follows:

$$[C_i, C_{ij}][S] = [C_i, C_{ij}](m_A^2, m_{H^\pm}^2, p_W^2, m_Z^2, m_S^2, m_W^2)$$

Diagram.2.5

$$M_{2.5}[h] = -\frac{e\alpha c_{\beta\alpha}^{-2}}{16\pi s_W^3} \{ B_0(m_{H^\pm}^2, m_W^2, m_h^2) + B_1(m_{H^\pm}^2, m_W^2, m_h^2) + [p_W^2 - 2m_{H^\pm}^2]C_1[h] \\ + 2C_{00}[h] + [m_{H^\pm}^2 - (p_W^2 - m_A^2)]C_{11}[h] - [p_W^2 - m_A^2 + m_{H^\pm}^2]C_{12}[h] \} \quad (\text{C.5})$$

$$M_{2.5}[H] = M_{2.5}[h][c_{\beta\alpha}^{-2} \rightarrow s_{\beta\alpha}^{-2}, m_h \rightarrow m_H, h \rightarrow H] \quad (\text{C.6})$$

$$M_{2.5}[A] = M_{2.5}[h][c_{\beta\alpha}^{-2} \rightarrow -1, m_h \rightarrow m_A, h \rightarrow A] \quad (\text{C.7})$$

Where the arguments of C_i and C_{ij} are as follows:

$$[C_i, C_{ij}][S] = [C_i, C_{ij}](m_A^2, m_{H^\pm}^2, p_W^2, m_{H^\pm}^2, m_W^2, m_S^2)$$

Diagram.2.6

$$M_{2.6}[h] = \frac{e\alpha c_{\beta\alpha^-} m_W}{8\pi c_W^2} g_{h^0 H^+ G^-} (2C_0[h] + C_1[h]) \quad (C.8)$$

$$M_{2.6}[H] = M_{2.6}[h][c_{\beta\alpha}^- \rightarrow -s_{\beta\alpha}^-, h \rightarrow H] \quad (C.9)$$

Where C_0 and C_1 have the same arguments as follows:

$$[C_0, C_1][S] = [C_0, C_1](m_A^2, m_{H^\pm}^2, p_W^2, m_Z^2, m_S^2, m_W^2)$$

Diagram.2.7

$$\begin{aligned} M_{2.7}[h] = & -\frac{e\alpha(c_W^2 - s_W^2)c_{\beta\alpha}^-^2}{16\pi s_W^3 c_W^2} \{B_0(m_{H^\pm}^2, m_Z^2, m_{H^\pm}^2) + B_1(m_{H^\pm}^2, m_Z^2, m_{H^\pm}^2) \\ & + [p_W^2 - m_h^2 - m_{H^\pm}^2]C_1[h] + 2C_{00}[h] + [-p_W^2 + m_A^2 + m_{H^\pm}^2]C_{11}[h] \\ & - [p_W^2 - m_A^2 + m_{H^\pm}^2]C_{12}[h]\} \end{aligned} \quad (C.10)$$

$$M_{2.7}[H] = M_{2.7}[h][c_{\beta\alpha}^- \rightarrow s_{\beta\alpha}^-, h \rightarrow H, m_h \rightarrow m_H] \quad (C.11)$$

The arguments of C_i and C_{ij} are given by :

$$[C_i, C_{ij}][S] = [C_i, C_{ij}](m_A^2, m_{H^\pm}^2, p_W^2, m_S^2, m_Z^2, m_{H^\pm}^2)$$

Diagram.2.8

$$M_{2.8}[h] = \frac{e\alpha s_{\beta\alpha^-} m_W}{8\pi s_W^2} g_{h^0 A^0 A^0} (2C_0[h] + C_1[h]) \quad (C.12)$$

$$M_{2.8}[H] = M_{2.8}[h][s_{\beta\alpha}^- \rightarrow c_{\beta\alpha}^-, h \rightarrow H, g_{h^0 A^0 A^0} \rightarrow g_{H^0 A^0 A^0}] \quad (C.13)$$

Where C_0 and C_1 have the same arguments:

$$[C_0, C_1][S] = [C_0, C_1](m_A^2, m_{H^\pm}^2, p_W^2, m_S^2, m_A^2, m_W^2)$$

Diagram.2.9

$$M_{2.9}[h] = \frac{e\alpha s_{\beta\alpha}^- m_W}{8\pi s_W^2} g_{h^0 H^+ H^-} (2C_0[h] + C_1[h]) \quad (C.14)$$

$$M_{2.9}[H] = M_{2.9}[h][s_{\beta\alpha}^- \rightarrow c_{\beta\alpha}^-, h \rightarrow H, g_{h^0 H^+ H^-} \rightarrow g_{H^0 H^+ H^-}] \quad (C.15)$$

Where C_0 and C_1 have the same arguments:

$$[C_0, C_1][S] = [C_0, C_1](m_A^2, m_{H^\pm}^2, p_W^2, m_W^2, m_{H^\pm}^2, m_S^2)$$

Diagram.2.10

$$M_{2.10}[Z] = -\frac{e\alpha(c_W^2 - s_W^2)m_W}{8\pi c_W^2} g_{A^0 H^+ G^-} (2C_0[Z] + C_1[Z]) \quad (C.16)$$

$$M_{2.10}[\gamma] = \frac{e\alpha m_W}{4\pi} g_{A^0 H^+ G^-} (2C_0[\delta] + C_1[\delta]) \quad (C.17)$$

Again the C_0 and C_1 have the same arguments:

$$[C_0, C_1][V] = [C_0, C_1](m_A^2, m_{H^\pm}^2, p_W^2, m_W^2, m_{H^\pm}^2, m_V^2)$$

Here δ is a small photon mass introduced to regularise the infrared divergence contained in the C_0 function.

Diagram.2.11

$$\begin{aligned} M_{2.11}[Z] = & \frac{e\alpha(c_W^2 - s_W^2)}{16\pi s_W^3} (4B_0(m_{H^\pm}^2, m_Z^2, m_{H^\pm}^2) + [2p_W^2 + m_A^2 - m_{H^\pm}^2 + 2m_W^2]2C_0[Z] \\ & + [4p_W^2 + 3(m_A^2 - m_{H^\pm}^2)]C_1[Z] + [p_W^2 + m_A^2 - m_{H^\pm}^2]4C_2[Z] - 4C_{00}[Z] \\ & + [p_W^2 - m_{H^\pm}^2 - 3m_A^2]C_{11}[Z] + [m_{H^\pm}^2 - m_A^2]2C_{12}[Z]) \end{aligned} \quad (C.18)$$

$$M_{2.11}[\gamma] = M_{2.11}[Z] \left[\frac{(c_W^2 - s_W^2)}{s_W^2} \rightarrow 2, m_Z \rightarrow \delta \right] \quad (C.19)$$

All C_i and C_{ij} have the same arguments

$$[C_i, C_{ij}][V] = [C_i, C_{ij}](m_A^2, m_{H^\pm}^2, p_W^2, m_W^2, m_{H^\pm}^2, m_V^2)$$

Diagram.2.12

$$M_{2.12}[h, Z] = -\frac{e\alpha c_{\beta\alpha}^{-2}}{16\pi s_W c_W^2} (2B_0(m_A^2, m_Z^2, m_h^2) + B_1(m_A^2, m_Z^2, m_h^2)) \quad (C.20)$$

$$M_{2.12}[H^+, W^+] = -\frac{e\alpha}{16\pi s_W^3} (2B_0(m_A^2, m_W^2, m_{H^\pm}^2) + B_1(m_A^2, m_W^2, m_{H^\pm}^2)) \quad (C.21)$$

$$M_{2.12}[H, Z] = -\frac{e\alpha s_{\beta\alpha}^{-2}}{16\pi s_W c_W^2} (2B_0(m_A^2, m_Z^2, m_H^2) + B_1(m_A^2, m_Z^2, m_H^2)) \quad (C.22)$$

Diagram.2.13

$$M_{2.13}[Z] = \frac{e\alpha(c_W^2 - s_W^2)}{16\pi s_W c_W^2} (B_0(m_{H^\pm}^2, m_{H^\pm}^2, m_Z^2) - B_1(m_{H^\pm}^2, m_{H^\pm}^2, m_Z^2)) \quad (\text{C.23})$$

$$M_{2.13}[\gamma] = -\frac{e\alpha}{8\pi s_W} (B_0(m_{H^\pm}^2, m_{H^\pm}^2, \delta) - B_1(m_{H^\pm}^2, m_{H^\pm}^2, \delta)) \quad (\text{C.24})$$

Diagram.2.14

$$M_{2.14} = -\frac{e\alpha}{16\pi s_W^3} (2B_0(m_{H^\pm}^2, m_W^2, m_A^2) + B_1(m_{H^\pm}^2, m_W^2, m_A^2)) \quad (\text{C.25})$$

Diagram 2.15 and 2.16

For this kind of topology, it is clear that the amplitude is proportional to the W gauge boson momentum (Lorentz invariance) and consequently for the W on-shell the amplitude vanishes.

$$M_{2.15} = 0 \quad , \quad M_{2.16} = 0 \quad (\text{C.26})$$

Appendix D: Gauge bosons and Higgs bosons self-energies

This appendix is devoted to the self-energies of the gauge bosons and Higgs bosons which are needed for the on-shell renormalisation scheme.

D.1 Photon self-energy

The photon self-energy $\Sigma^{\gamma\gamma}$ can be cast in three parts: i) fermions Diagram 2.17: $\Sigma_f^{\gamma\gamma}$, ii) pure Standard Model diagrams 2.19 , 2.20 , 2.21 , 2.22, 2.24 and 2.25: $\Sigma_{SM}^{\gamma\gamma}$ and iii) pure THDM contribution 2.18 and 2.23: $\Sigma_{THDM}^{\gamma\gamma}$. We then have:

$$\Sigma^{\gamma\gamma}(q^2) = \Sigma_f^{\gamma\gamma} + \Sigma_{SM}^{\gamma\gamma} + \Sigma_{THDM}^{\gamma\gamma} \quad (\text{D.1})$$

with

$$\Sigma_f^{\gamma\gamma}(q^2) = -\frac{\alpha N_C Q_f^2}{\pi} (A_0(m_f^2) + q^2 B_1(q^2, m_f^2, m_f^2) - 2B_{00}(q^2, m_f^2, m_f^2)) \quad (\text{D.2})$$

$$\Sigma_{THDM}^{\gamma\gamma}(q^2) = -\frac{\alpha}{2\pi} [2B_{00}(q^2, m_{H^\pm}^2, m_{H^\pm}^2) - A_0(m_{H^\pm}^2)] \quad (\text{D.3})$$

$$\begin{aligned} \Sigma_{SM}^{\gamma\gamma}(q^2) &= \frac{\alpha}{12\pi} [12m_W^2 - 2q^2 - 6A_0(m_W^2) - 12q^2 B_0 - 36B_{00}] \\ &\quad + \frac{\alpha}{\pi} [-m_W^2 + 2A_0(m_W^2)] \end{aligned} \quad (\text{D.4})$$

The arguments of B_0 , B_1 and B_{00} are given by: $[B_0, B_1, B_{00}](q^2, m_W^2, m_W^2)$

D.2 Z-Photon mixing self-energy

In a similar way, the Z-photon mixing self-energy can be cast into three parts: i) fermion diagram 2.26: $\Sigma_f^{Z\gamma}$, ii) pure Standard Model diagrams 2.28; 2.29, 2.30, 2.31, 2.33 and 2.34: $\Sigma_{SM}^{Z\gamma}$ and iii) pure THDM contribution 2.27 and 2.32: $\Sigma_{THDM}^{Z\gamma}$. We then have:

$$\Sigma^{Z\gamma}(q^2) = \Sigma_f^{Z\gamma} + \Sigma_{SM}^{Z\gamma} + \Sigma_{THDM}^{Z\gamma} \quad (D.5)$$

with

$$\Sigma_f^{Z\gamma}(q^2) = \frac{\alpha N_C Q_f}{2\pi} (g_Z^{fL} + g_Z^{fR}) \{ A_0(m_f^2) + q^2 B_1(q^2, m_f^2, m_f^2) - 2B_{00}(q^2, m_f^2, m_f^2) \} \quad (D.6)$$

$$\Sigma_{THDM}^{Z\gamma}(q^2) = -\frac{\alpha}{4\pi c_W s_W} (c_W^2 - s_W^2) [2B_{00}(q^2, m_{H^\pm}^2, m_{H^\pm}^2) - A_0(m_{H^\pm}^2)] \quad (D.7)$$

$$\Sigma_{SM}^{Z\gamma}(q^2) = \frac{\alpha}{12\pi c_W s_W} \{ (c_W^2 (12m_W^2 - 2q^2 - 6A_0(m_W^2)) - (6m_W^2 + 15c_W^2 q^2) B_0 + (6s_W^2 - 30c_W^2) B_{00} - 6c_W^2 q^2 B_1) + 3(-4c_W^2 m_W^2 + (7c_W^2 - s_W^2) A_0(m_W^2)) \} \quad (D.8)$$

The arguments of B_0 , B_1 and B_{00} are given by: $[B_0, B_1, B_{00}](q^2, m_W^2, m_W^2)$. Where

$$\begin{aligned} g_Z^{uL} &= -\frac{(1 - 2s_W^2 e_u)}{2s_W c_W}, & g_Z^{fR} &= \frac{s_W^2 e_f}{s_W c_W} \\ g_Z^{dL} &= \frac{(1 + 2s_W^2 e_d)}{2s_W c_W} \\ \text{for quarks:} & & e_u &= -2e_d = \frac{2}{3}|e| \\ \text{for leptons:} & & e_u &= 0, \quad e_d = -|e|. \end{aligned} \quad (D.9)$$

D.3 Z-Z self-energy

In a similar way, the Z self-energy can be cast into three parts: i) fermion diagram 2.35: Σ_f^{ZZ} , ii) pure Standard Model diagrams 2.37, 2.38, 2.41, 2.42, 2.44 and 2.45: Σ_{SM}^{ZZ} and iii) pure THDM contribution 2.36, 2.39, 2.40 and 2.43: Σ_{THDM}^{ZZ} . We then have:

$$\Sigma^{ZZ}(q^2) = \Sigma_f^{ZZ}(q^2) + \Sigma_{SM}^{ZZ}(q^2) + \Sigma_{THDM}^{ZZ}(q^2) \quad (D.10)$$

with:

$$\Sigma_{ff}^{ZZ}(q^2) = -\frac{\alpha N_C}{2\pi} \{ m_f^2 [g_Z^{fL} - g_Z^{fR}]^2 B_0(q^2, m_f^2, m_f^2) + (g_Z^{fL^2} + g_Z^{fR^2}) (A_0(m_f^2) - 2B_{00}(q^2, m_f^2, m_f^2) + q^2 B_1(q^2, m_f^2, m_f^2)) \} \quad (D.11)$$

$$\begin{aligned} \Sigma_{THDM}^{ZZ}(q^2) &= \frac{\alpha}{4\pi c_W^2 s_W^2} \{ m_Z^2 s_{\beta\alpha}^{-2} B_0(q^2, m_h^2, m_Z^2) + c_{\beta\alpha}^{-2} m_Z^2 B_0(q^2, m_H^2, m_Z^2) \\ &\quad - c_{\beta\alpha}^{-2} B_{00}(q^2, m_h^2, m_A^2) - s_{\beta\alpha}^{-2} B_{00}(q^2, m_h^2, m_Z^2) - s_{\beta\alpha}^{-2} B_{00}(q^2, m_H^2, m_A^2) \\ &\quad - c_{\beta\alpha}^{-2} B_{00}(q^2, m_H^2, m_Z^2) - (c_W^2 - s_W^2)^2 B_{00}(q^2, m_{H^\pm}^2, m_{H^\pm}^2) \} + \\ &\quad \frac{\alpha}{16\pi c_W^2 s_W^2} \{ A_0(m_A^2) + A_0(m_h^2) + A_0(m_H^2) + 2(c_W^2 - s_W^2)^2 A_0(m_{H^\pm}^2) \} \end{aligned}$$

$$\begin{aligned}
\Sigma_{SM}^{ZZ}(q^2) = & \frac{\alpha}{12\pi c_W^2 s_W^2} \{ c_W^4 (12m_W^2 - 2q^2 - 6A_0(m_W^2)) - (27c_W^4 - 6c_W^2 s_W^2 + 3s_W^4) B_{00} \\
& - (6c_W^4 m_W^2 + 15c_W^4 q^2 - 6m_W^2 s_W^4) B_0 - 6c_W^4 q^2 B_1 \} \\
& - \frac{\alpha}{16\pi c_W^2 s_W^2} \{ 16c_W^4 m_W^2 - (26c_W^4 - 4c_W^2 s_W^2 + 2s_W^4) A_0(m_W^2) - A_0(m_Z^2) \}
\end{aligned} \tag{D.12}$$

The arguments of B_0 , B_1 and B_{00} are given as follows : $[B_0, B_1, B_{00}](q^2, m_W^2, m_Z^2)$

D.4 W-W self-energy

The W self-energy can also be cast into three parts: i) fermion diagram 2.46: Σ_f^{WW} , ii) pure Standard Model diagrams 2.50 \rightarrow 2.54 and 2.56: Σ_{SM}^{WW} and iii) pure THDM contribution 2.47 \rightarrow 2.49 and 2.55: Σ_{THDM}^{WW} . Then we have:

$$\Sigma^{WW}(q^2) = \Sigma_f^{WW}(q^2) + \Sigma_{SM}^{WW}(q^2) + \Sigma_{THDM}^{WW}(q^2) \tag{D.13}$$

with:

$$\begin{aligned}
\Sigma_{ff'}^{WW}(q^2) = & \frac{\alpha N_C}{4\pi s_W^2} (2B_{00}(q^2, m_{f'}^2, m_f^2) - A_0(m_f^2) - m_{f'}^2 B_0(q^2, m_{f'}^2, m_f^2) \\
& - q^2 B_1(q^2, m_{f'}^2, m_f^2))
\end{aligned} \tag{D.14}$$

$$\begin{aligned}
\Sigma_{2HDM}^{WW}(q^2) = & \frac{\alpha}{4\pi s_W^2} (m_W^2 s_{\beta\alpha}^2 B_0(q^2, m_h^2, m_W^2) + c_{\beta\alpha}^2 m_W^2 B_0(q^2, m_H^2, m_W^2) \\
& - B_{00}(q^2, m_{H^\pm}^2, m_A^2) - c_{\beta\alpha}^{-2} B_{00}(q^2, m_{H^\pm}^2, m_h^2) - s_{\beta\alpha}^{-2} B_{00}(q^2, m_{H^\pm}^2, m_H^2) \\
& - s_{\beta\alpha}^{-2} B_{00}(q^2, m_W^2, m_h^2) - c_{\beta\alpha}^{-2} B_{00}(q^2, m_W^2, m_H^2)) + \frac{\alpha}{16\pi s_W^2} (A_0(m_A^2) \\
& + A_0(m_h^2) + A_0(m_H^2) + 2A_0(m_{H^\pm}^2))
\end{aligned} \tag{D.15}$$

$$\begin{aligned}
\Sigma_{SM}^{WW}(q^2) = & \frac{\alpha}{12\pi c_W^2 s_W^2} (2c_W^4 (3m_W^2 + 3m_Z^2 - q^2 - 3A_0(m_Z^2)) + c_W^2 (6m_W^2 s_W^2 - 2q^2 s_W^2) \\
& - (3c_W^2 m_W^2 s_W^2 + 15c_W^2 q^2 s_W^2) B_0(q^2, \delta, m_W^2) + (3m_W^2 s_W^4 - 6c_W^4 m_W^2 - 15c_W^4 q^2) B_0 \\
& - 24c_W^2 s_W^2 B_{00}(q^2, m_W^2, \delta) - (3c_W^2 + 24c_W^4) B_{00} - 6c_W^2 q^2 s_W^2 B_1(q^2, m_W^2, \delta) \\
& - 6c_W^4 q^2 B_1) + \frac{\alpha}{16\pi s_W^2} (-8m_W^2 - 8c_W^2 m_Z^2 + 14A_0(m_W^2) \\
& + (1 + 12c_W^2) A_0(m_Z^2))
\end{aligned} \tag{D.16}$$

The arguments of B_0 , B_1 and B_{00} are given by :

$$[B_0, B_1, B_{00}](q^2, m_W^2, m_Z^2)$$

D.5 CP-odd Higgs boson self-energy

The CP-odd Higgs self-energy Σ^{AA} can be cast into three parts: i) fermionic part 2.61, ii) pure scalar part 2.62; 2.63, 2.64 and 2.67 iii) mixing of gauge boson and scalar 2.65, 2.66, 2.68 and 2.69 in such a way that:

$$\Sigma^{AA}(q^2) = \Sigma_f^{AA}(q^2) + \Sigma_S^{AA}(q^2) + \Sigma_{VS}^{AA}(q^2) \tag{D.17}$$

with

$$\Sigma_f^{AA}(q^2) = -\frac{\alpha N_C}{\pi} Y_{ff}^2 (A_0(m_f^2) + q^2 B_1(q^2, m_f^2, m_f^2)) \quad (D.18)$$

$$\begin{aligned} \Sigma_S^{AA}(q^2) = & \frac{\alpha}{4\pi} (g_{hAA}^2 B_0(q^2, m_A^2, m_h^2) + g_{HAA}^2 B_0(q^2, m_A^2, m_H^2) \\ & + g_{hAG}^2 B_0(q^2, m_h^2, m_Z^2) + g_{HAG}^2 B_0(q^2, m_H^2, m_Z^2) \\ & + 2g_{AH+G-}^2 B_0(q^2, m_{H^\pm}^2, m_W^2)) + \frac{\alpha}{8\pi} (-g_{AAAA} A_0(m_A^2) - g_{hhAA} A_0(m_h^2) \\ & - g_{HHAA} A_0(m_H^2) - 2g_{H+H-AA} A_0(m_{H^\pm}^2) - 2g_{G+G-AA} A_0(m_W^2) \\ & - g_{AAGG} A_0(m_Z^2) + \frac{2}{s_W^2 c_W^2} A_0(m_Z^2) + \frac{4}{s_W^2} A_0(m_W^2) - \frac{2}{s_W^2} m_W^2 - \frac{1}{s_W^2 c_W^2} m_Z^2) \end{aligned} \quad (D.19)$$

$$\begin{aligned} \Sigma_{SV}^{AA}(q^2) = & -\frac{\alpha}{16\pi c_W^2 s_W^2} (c_{\beta\alpha}^{-2} (A_0(m_Z^2) + (m_h^2 + q^2) B_0(q^2, m_h^2, m_Z^2) \\ & - 2q^2 B_1(q^2, m_h^2, m_Z^2)) + s_{\beta\alpha}^{-2} (A_0(m_Z^2) + (m_H^2 + q^2) B_0(q^2, m_H^2, m_Z^2) \\ & - 2q^2 B_1(q^2, m_H^2, m_Z^2)) + c_W^2 (A_0(m_W^2) + (m_{H^\pm}^2 + q^2) B_0(q^2, m_{H^\pm}^2, m_W^2) \\ & - 2q^2 B_1(q^2, m_{H^\pm}^2, m_W^2))) \end{aligned} \quad (D.20)$$

D.6 Charged Higgs boson self-energy

The charged Higgs boson self-energy $\Sigma^{H^+H^-}$ can be cast into three parts: i) fermionic part 2.70, ii) pure scalar part 2.71; 2.72, 2.73 and 2.76 iii) mixing of gauge boson and scalar 2.74, 2.75 and 2.77 in such a way that:

$$\Sigma^{H^+H^-}(q^2) = \Sigma_f^{H^\pm H^\pm}(q^2) + \Sigma_S^{H^+H^-}(q^2) + \Sigma_{VS}^{H^+H^-}(q^2) \quad (D.21)$$

$$\begin{aligned} \Sigma_{ff'}^{H^\pm H^\pm}(q^2) = & -\frac{\alpha N_C}{2\pi} ((Y_{ff'}^L)^2 + (Y_{ff'}^R)^2) (A_0(m_f^2) + q^2 B_1(q^2, m_{f'}^2, m_f^2)) \\ & + (m_{f'}^2 (Y_{ff'}^L)^2 + Y_{ff'}^R)^2 + 2m_{f'} m_f Y_{ff'}^L Y_{ff'}^R) B_0(q^2, m_{f'}^2, m_f^2) \end{aligned} \quad (D.22)$$

$$\begin{aligned} \Sigma_S^{H^\pm H^\pm}(q^2) = & \frac{\alpha}{4\pi} (g_{AH+G-}^2 B_0(q^2, m_A^2, m_W^2) + g_{hH+H-}^2 B_0(q^2, m_h^2, m_{H^\pm}^2) \\ & + g_{hH+G-}^2 B_0(q^2, m_h^2, m_W^2) + g_{HH+H-}^2 B_0(q^2, m_H^2, m_{H^\pm}^2) \\ & + g_{HH+G-}^2 B_0(q^2, m_H^2, m_W^2)) - \frac{\alpha}{8\pi} (g_{H+H-AA} A_0(m_A^2) + g_{H+H-hh} A_0(m_h^2) \\ & + g_{H+H-HH} A_0(m_H^2) + 2g_{H+H-H+H-} A_0(m_{H^\pm}^2) + \frac{2}{s_W^2} (m_W^2 - 2A_0(m_W^2)) \\ & + g_{H+H-GG} A_0(m_Z^2) + \frac{(s_W^2 - c_W^2)^2}{c_W^2 s_W^2} (m_Z^2 - 2A_0(m_Z^2))) \end{aligned} \quad (D.23)$$

$$\begin{aligned} \Sigma_V^{H^\pm H^\pm}(q^2) = & -\frac{\alpha}{16\pi s_W^2} (4s_W^2 ((m_{H^\pm}^2 + q^2) B_0(q^2, 0, m_{H^\pm}^2) - 2q^2 B_1(q^2, m_{H^\pm}^2, 0)) \\ & + \frac{(c_W^2 - s_W^2)^2}{c_W^2} (A_0(m_Z^2) + (m_{H^\pm}^2 + q^2) B_0(q^2, m_{H^\pm}^2, m_Z^2) \\ & - 2q^2 B_1(q^2, m_{H^\pm}^2, m_Z^2)) + (A_0(m_A^2) + (m_W^2 + 4q^2) B_0(q^2, m_A^2, m_W^2) \\ & + 4q^2 B_1(q^2, m_W^2, m_A^2)) + c_{\beta\alpha}^{-2} (A_0(m_h^2) + (m_W^2 + 4q^2) B_0(q^2, m_h^2, m_W^2) \\ & + 4q^2 B_1(q^2, m_W^2, m_h^2)) + s_{\beta\alpha}^{-2} (A_0(m_H^2) + (m_W^2 + 4q^2) B_0(q^2, m_H^2, m_W^2) \end{aligned}$$

$$+4q^2 B_1(q^2, m_W^2, m_H^2))) \quad (\text{D.24})$$

References

- [1] J.F. Gunion, H.E. Haber, G.L. Kane and S. Dawson, *The Higgs Hunter's Guide* (Addison–Wesley, Reading, 1990).
- [2] S. Weinberg, Phys. Rev. Lett. **19** (1967) 1264; S. Glashow, Nucl. Phys. **20** (1961) 579; A. Salam, in *Elementary Particle Theory*, ed. N. Svartholm, (1968) p367.
- [3] J. Preskill, S.P. Trivedi, F. Wilczek and M.B. Wise, Nucl. Phys. **B363** (1991) 207.
- [4] S. Komamiya, Phys. Rev. **D38** (1988) 2158; A. Sopczak, Z.Phys. **C65** (1995) 449; S. Moretti and K. Odagiri, J. Phys. **G23** (1997) 537; A. Arhrib, M. Capdequi Peyranère and G. Moultaka, Phys. Lett. **B341** (1995) 313; M.A. Diaz and Tonnis A. ter Veldhuis, hep-ph/9501315; A. Gutierrez-Rodriguez and O.A. Sampayo, hep-ph/9911361;
- [5] A. Arhrib and G. Moultaka, Nucl. Phys. **B558** (1999) 3.
- [6] E. Eichten, I. Hinchliffe, K. Lane and C. Quigg, Rev. Mod. Phys. **56** (1984) 579; J. Gunion, H.E. Haber, F.E. Paige, W.K. Tung and S.S.D. Willenbrock, Nucl. Phys. **B294** (1987) 621; R.M. Barnett, H.E. Haber and D.E. Soper, Nucl. Phys. **B306** (1988) 697; D.A. Dicus, J.L. Hewett, C. Kao, and T.G. Rizzo, Phys. Rev. **D40** (1989) 787; V. Barger, R.J.N. Philips and D.P. Roy, Phys. Lett. **B324** (1994) 236; J.L. Diaz–Cruz and O.A. Sampayo, Phys. Rev. **D50** (1994) 6820.
- [7] Jiang Yi, Ma Wen-Gan, Han Liang, Han Meng and Yu Zeng-hui; J. Phys. **G24** (1998) 83; J. Phys. **G23** (1997) 385, erratum-ibid. **G23** (1997) 1151; A. Krause, T. Plehn, M. Spira and P.W. Zerwas, Nucl. Phys. **B519** (1998) 85; S. Moretti and K. Odagiri, Phys. Rev. **D55** (1997) 5627; Li Gang Jin, Chong Sheng Li, R.J. Oakes and Shou Hua Zhu, hep-ph/9907482; A.A. Barrientos Bendezu and B.A. Kniehl, hep-ph/9908385; O. Brein and W. Hollik, hep-ph/9908529.
- [8] K. Odagiri, Phys. Lett. **B452** (1999) 327; K. Odagiri, hep-ph/9901432; D.P. Roy, Phys. Lett. **B459** (1999) 607; F. Borzumati, J.L. Kneur and N. Polonsky, Phys. Rev. **D60** (1999) 115011; D.J. Miller, S. Moretti, D.P. Roy and W.J. Stirling, Phys. Rev. **D61** (2000) 055011; S. Moretti and D.P. Roy, Phys. Lett. **B470** (1999) 209.
- [9] V. Barger *et al.*, Phys. Rep. **286** (1997) 1; R. Alanakyan, hep-ph/9804247; A.G. Akeroyd, A. Arhrib and C. Dove, Phys. Rev. **D61** (2000) 071702.
- [10] D. Bowser-Chao *et al.*, Phys. Lett. **B315** (1995) 313; W.G. Ma *et al.*, Phys. Rev. **D53** (1996) 1304; Shou Hua Zhu, Chong Sheng Li and Choung Shou Gao, Phys. Rev. **D58** (1998) 055007.
- [11] Combined Experimental Limits; ALEPH 99-081 CONF 99-052; DELPHI 99-142 CONF 327; L3 Note 2442; OPAL Technical Note TN-614.

- [12] M. Drees, E.A. Ma, P.N. Pandita, D.P. Roy and S.K. Vempati, Phys. Lett. **B433** (1998) 346.
- [13] D0 Collaboration, B. Abbott *et al.* Phys. Rev. Lett. **82** (1999) 4975; CDF Collaboration, F. Abe *et al.*, Phys. Rev. Lett. **79** (1997) 357.
- [14] A. Djouadi, J. Kalinowski and P.M. Zerwas, Z. Phys. **C70** (1996) 435.
- [15] A. Djouadi, J. Kalinowski, P. Ohmann and P.M. Zerwas, Z. Phys. **C74** (1997) 93.
- [16] A. Pilaftsis, Phys. Lett. **B435** (1998) 88; Phys. Rev. **D58** (1998) 096010; A. Pilaftsis and C.E.M. Wagner, Nucl. Phys. **B553** (1999) 3; D.A. Demir, Phys. Rev. **D60** (1999) 055006; S.Y. Choi and Jae Sik Lee, Phys. Rev. **D61** (2000) 015003.
- [17] A.G. Akeroyd, Nucl. Phys. **B544** (1999) 557.
- [18] F.M. Borzumati and A. Djouadi, hep-ph/9806301.
- [19] A.G. Akeroyd, A. Arhrib and E. Naimi, Eur. Phys. J. **C12** (2000) 451.
- [20] K. Hoffman (OPAL Collaboration), private communication.
- [21] M. Ciuchini, G. Degrassi, P. Gambino and G.F. Giudice, Nucl. Phys. **B527** (1998) 21.
- [22] F.M. Borzumati and C. Greub, PM/98/23, hep-ph/9810240; Phys. Rev. **D58** 074004 (1998); Phys. Rev. **D59** 057501 (1999).
- [23] M. Drees, M. Guchait and D.P. Roy, Phys. Lett. **B471** (2000) 39.
- [24] G. 't Hooft and M. Veltman, Nucl. Phys. **B44** (1972) 189;
P. Breitenlohner and D. Maison, Commun. Math. Phys. **52** (1977) 11.
- [25] H.Eck and J. Kublbeck, Guide to FeynArts 1.0, University of Wurzburg, 1992.
- [26] R.Mertig, Guide to FeynCalc 1.0, University of Wurzburg, 1992.
- [27] G. Passarino and M. Veltman, Nucl. Phys. **B160** (1979) 151;
G. 't Hooft and M. Veltman, Nucl. Phys. **B153** (1979) 365.
- [28] G.J. van Oldenborgh, Comput.Phys.Comm. **66** (1991) 1.
- [29] A. Denner, Fortsch. Phys. **41**: 307-420, 1993.
- [30] A. Arhrib, Thèse d'Etat, University Cadi Ayyad (Marakesh, Morocc) Unpublished;
A. Kraft, PhD Thesis , University of Karlsruhe (Germany) Unpublished.
- [31] L. Brucher and R. Santos, Eur. Phys. J **C12** (2000) 87.
- [32] A. Denner, R.J. Guth, W. Hollik and J.H. Kuhn, Z. Phys. **C51** (1991) 695.
- [33] J. Erler and P. Langacker, talk given at the 5th International Wein Symposium (WEIN 98), Santa Fe, Jun 1998 (hep-ph/9809352).

- [34] V. Berger et al, Phys. Rev. **D41** (1990) 3421; Y. Grossman, Nucl. Phys. **B355** (1994) 426.
- [35] M. Krawczyk, hep-ph/9803484, Presented at Workshop on Physics at the First Muon Collider and at the Front End of the Muon Collider, Batavia, IL, 6-9 Nov 1997. see also hep-ph/9812536 M. Krawczyk, J. Zochowski and P. Mattig, DESY-98-177, Eur. Phys. J **C8** (1999) 495.
- [36] R. Casalbuoni, D. Dominici, F. Feruglio and R. Gatto Phys. Lett. **B200** (1988) 495; J. Maalampi, J. Sirkka and I. Vilja, Phys.Lett. **B265** (1991) 371; S. Kanemura, T. Kubota and E.Takasugi, Phys. Lett. **B313** (1993) 155.
- [37] A. Akeroyd, A. Arhrib and E. Naimi, in preparation
- [38] C. Caso et al, Eur. Phys. J **C3** (1998) 1.
- [39] S. Eidelman and F. Jegerlehner, Z. Phys. **C67** (1995) 585; H. Burkhardt and B. Pietrzyk, Phys. Lett. **B356** (1995) 398.
- [40] A. Arhrib, M. Capdequi Peyranère, W. Hollik and G. Moultaka, hep-ph/9912527; S. Kanemura, hep-ph/9911541; S.H Zhu hep-ph/9901221.
- [41] S. Kanemura, T. Kasai and Y. Okada, Phys. Lett. **B471** (1999) 182.

Figure Captions

Fig. 1 Lowest-order Feynman diagram for the decay $H^+ \rightarrow A^0 W^+$.

Fig. 2 Feynman diagrams for the one-loop corrections to the decay $H^+ \rightarrow A^0 W^+$: i) vertex (2.1 \rightarrow 2.16), ii) gauge boson self-energies γ - γ (2.17 \rightarrow 2.25), γ -Z (2.26 \rightarrow 2.34), Z-Z (2.35 \rightarrow 2.45) and W-W (2.46 \rightarrow 2.56), iii) Bremsstrahlung diagrams for $H^+ \rightarrow A^0 W^+ \gamma$: Fig. 2.57 \rightarrow 2.60 iv) Charged Higgs boson self-energy (2.61 \rightarrow 2.69) and CP-odd Higgs boson self-energy (2.70 \rightarrow 2.77).

Fig. 3 Total contribution to Γ_H as function of m_{H^\pm} . We chose: $m_H = m_{H^\pm} - 10$, $m_h = 120$, $m_A = 150$ (GeV), $\alpha = \beta - \frac{\pi}{2}$.

Fig.3.a: $\tan \beta = 0.5$, for four values of $\lambda_5 = 0.0, 2.0, 6.0$ and 8.5 .

Fig.3.b: $\tan \beta = 1.5$, for four values of $\lambda_5 = 0.0, 2.0, 4.0$ and 6.5 .

Fig. 4 Total contribution to Γ_H as function of m_A . We chose: $m_H = 504$, $m_h = 359$, $m_{H^\pm} = 534$ (GeV) and $\alpha = \beta - \frac{\pi}{2}$.

Fig.4.a: $\tan \beta = 0.8$, for four values of $\lambda_5 = 0.0, 4.0, 6.0$ and 10.0 .

Fig.4.b: $\tan \beta = 1.6$, for four values of $\lambda_5 = 0.0, 4.0, 8.0$ and 12.0 .

Fig. 5 Total contribution to Γ_H as function of λ_5 . We chose: $m_H = 177$, $m_h = 120$, $m_{H^\pm} = 202$, $m_A = 112$ (GeV), $\alpha = \beta - \frac{\pi}{2}$, and several values of $\tan \beta$.

Fig. 6 Ratio R (eq 5.1) as a function of $\tan \beta$ for various values of $m_{H^\pm} = 300, 400, 500, 600$ (GeV) and for $m_A = 70$ GeV.

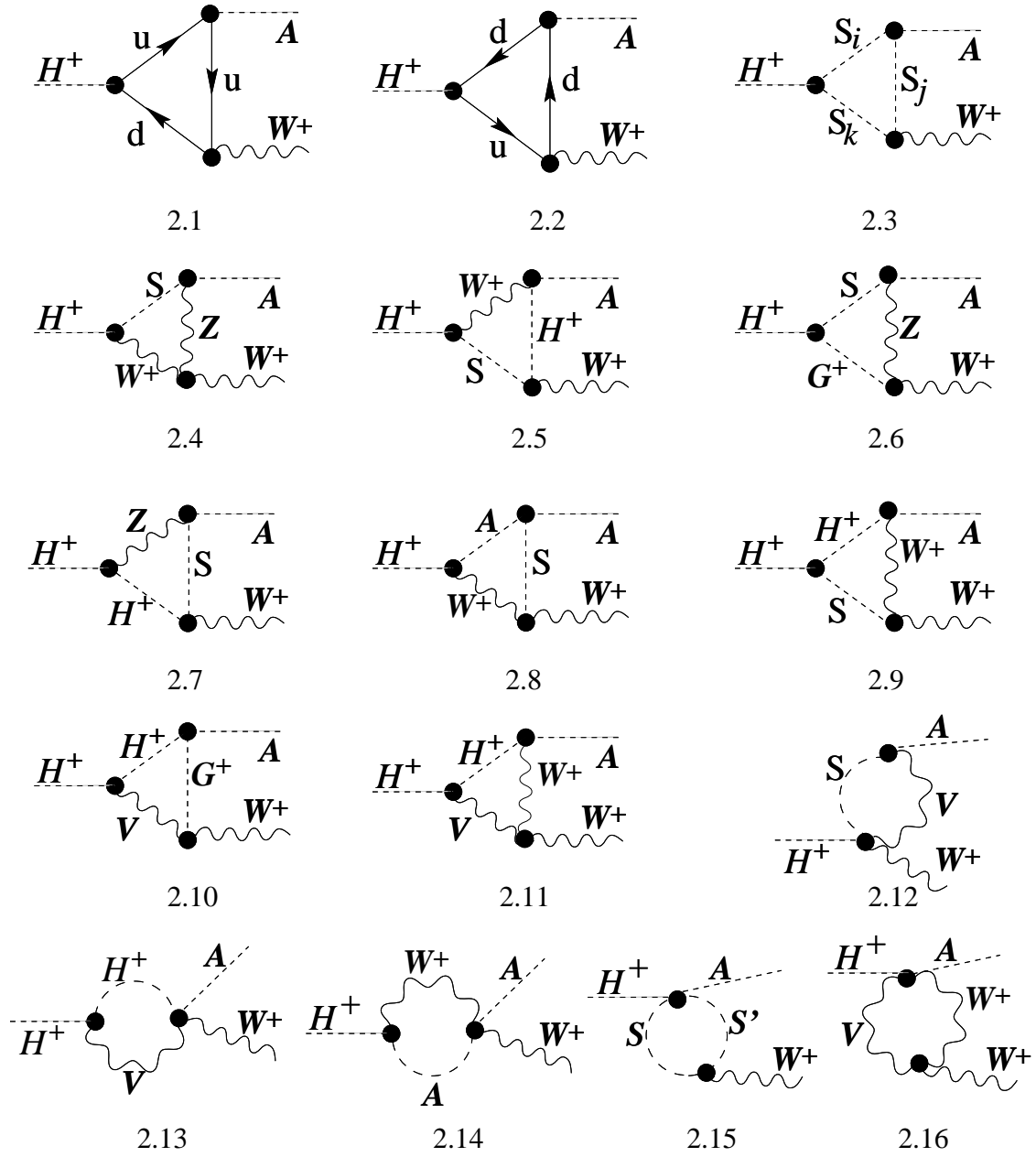
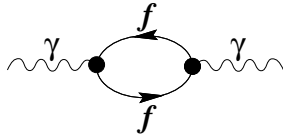
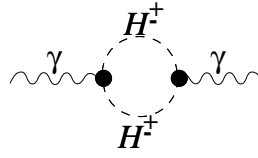


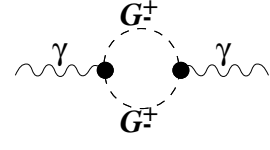
Figure. 2



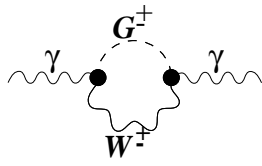
2.17



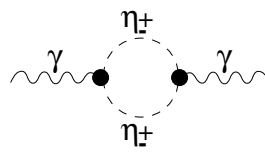
2.18



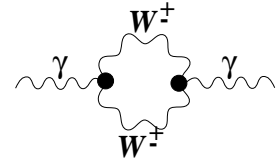
2.19



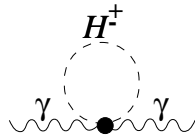
2.20



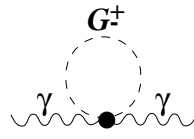
2.21



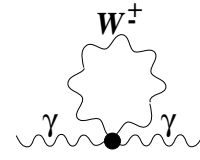
2.22



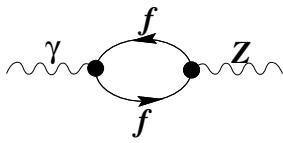
2.23



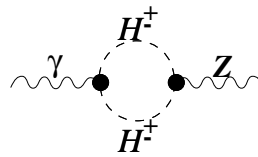
2.24



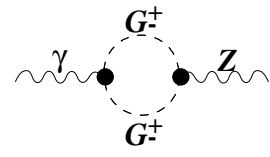
2.25



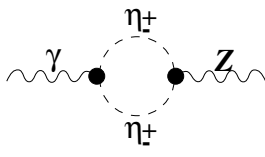
2.26



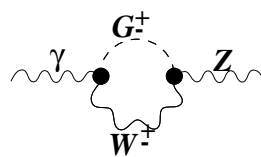
2.27



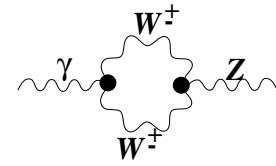
2.28



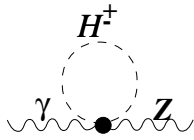
2.29



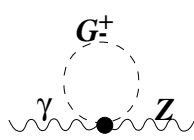
2.30



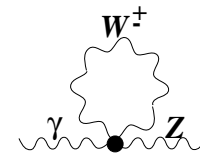
2.31



2.32

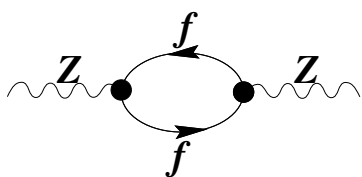


2.33

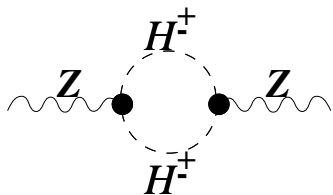


2.34

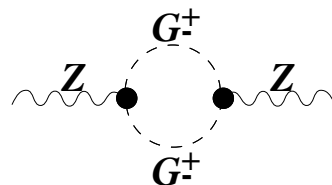
Figure. 2 (Cont.)



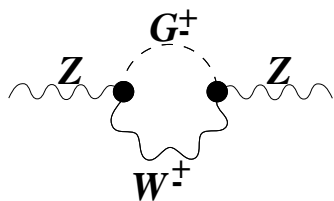
2.35



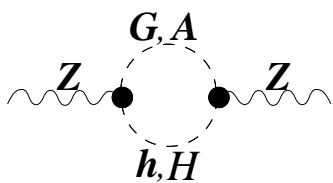
2.36



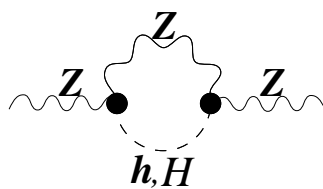
2.37



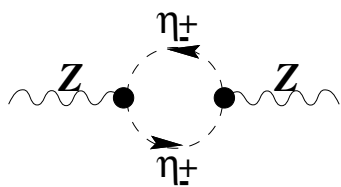
2.38



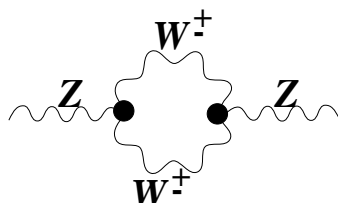
2.39



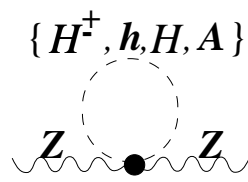
2.40



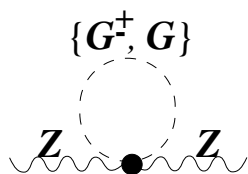
2.41



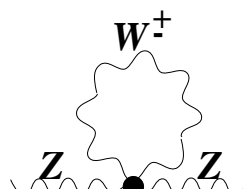
2.42



2.43



2.44



2.45

Figure. 2 (Cont.)

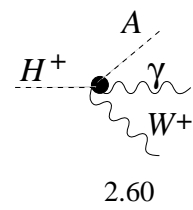
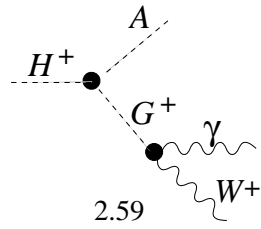
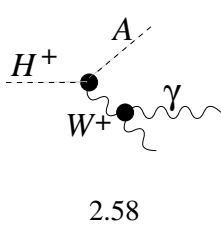
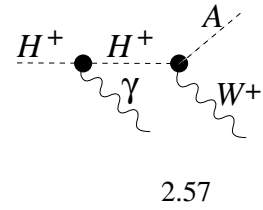
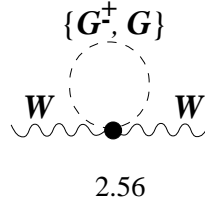
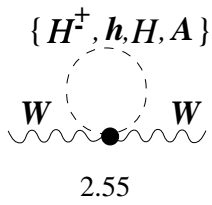
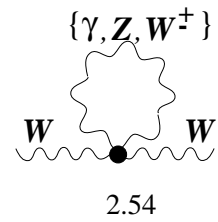
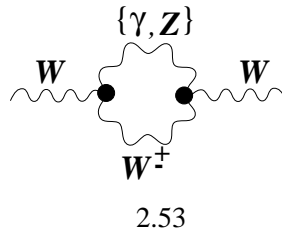
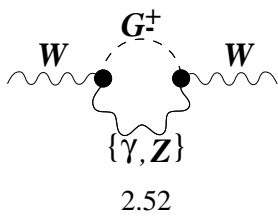
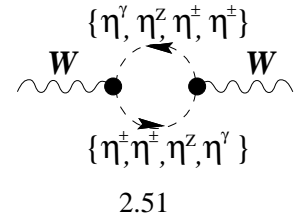
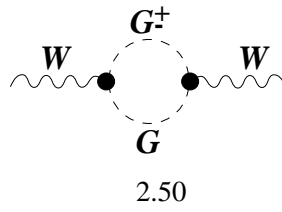
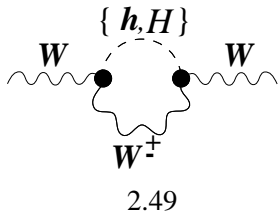
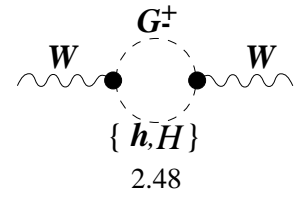
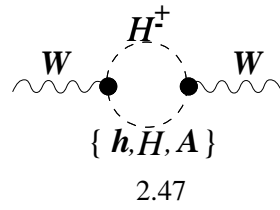
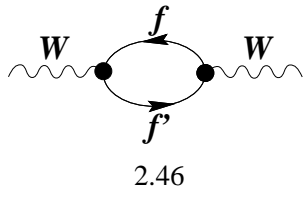
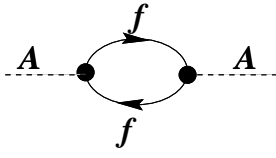
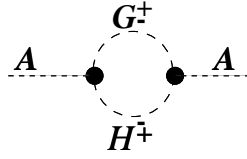


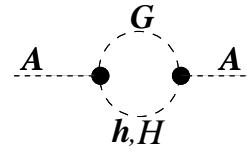
Figure . 2 (Cont.)



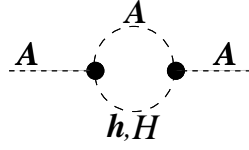
2.61



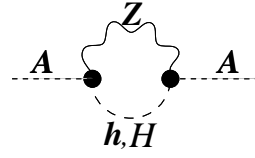
2.62



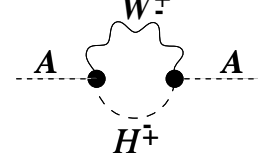
2.63



2.64

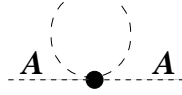


2.65

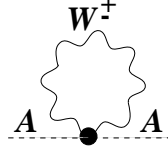


2.66

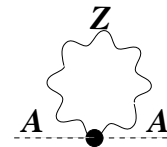
$\{H^+, G^+, h, H, A, G\}$



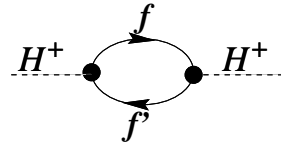
2.67



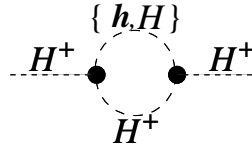
2.68



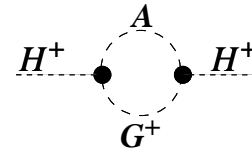
2.69



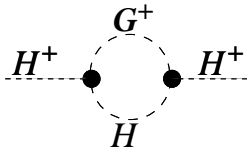
2.70



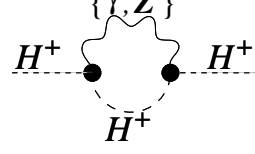
2.71



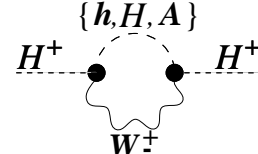
2.72



2.73

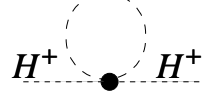


2.74



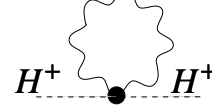
2.75

$\{H^+, h, H, A, G\}$



2.76

$\{\gamma, Z, W^+\}$



2.77

Figure . 2 (cont.)

Figure. 3. a

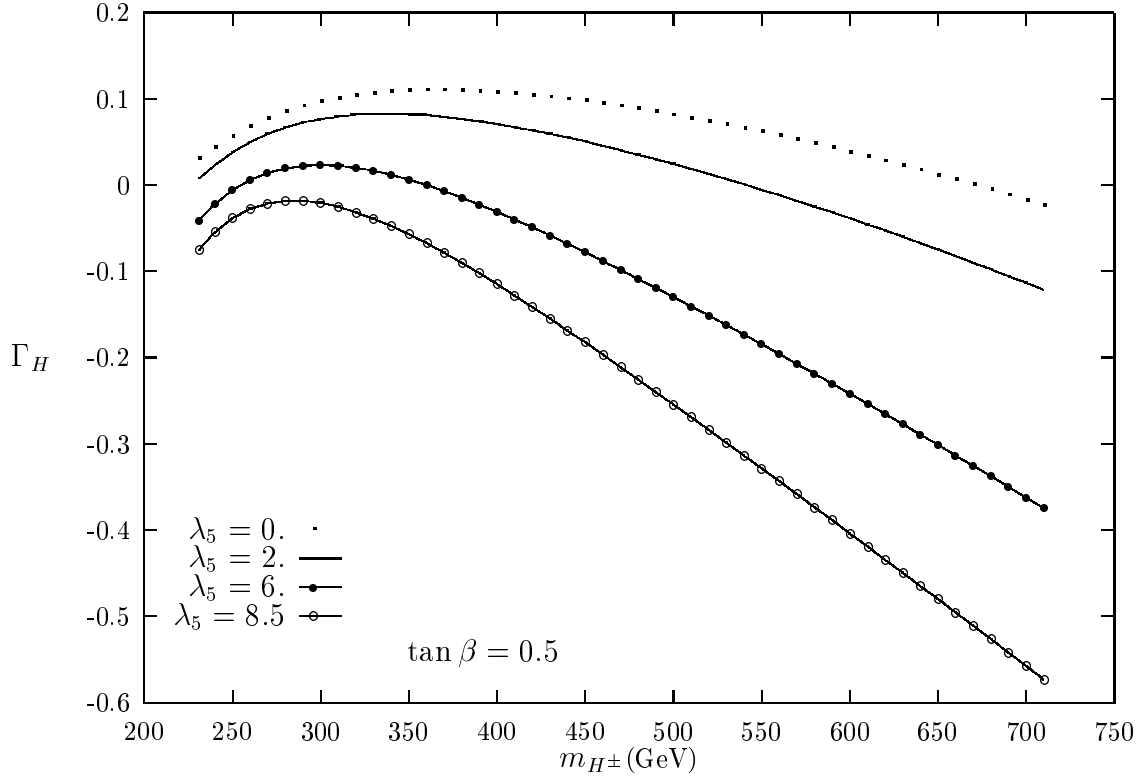


Figure. 3.b

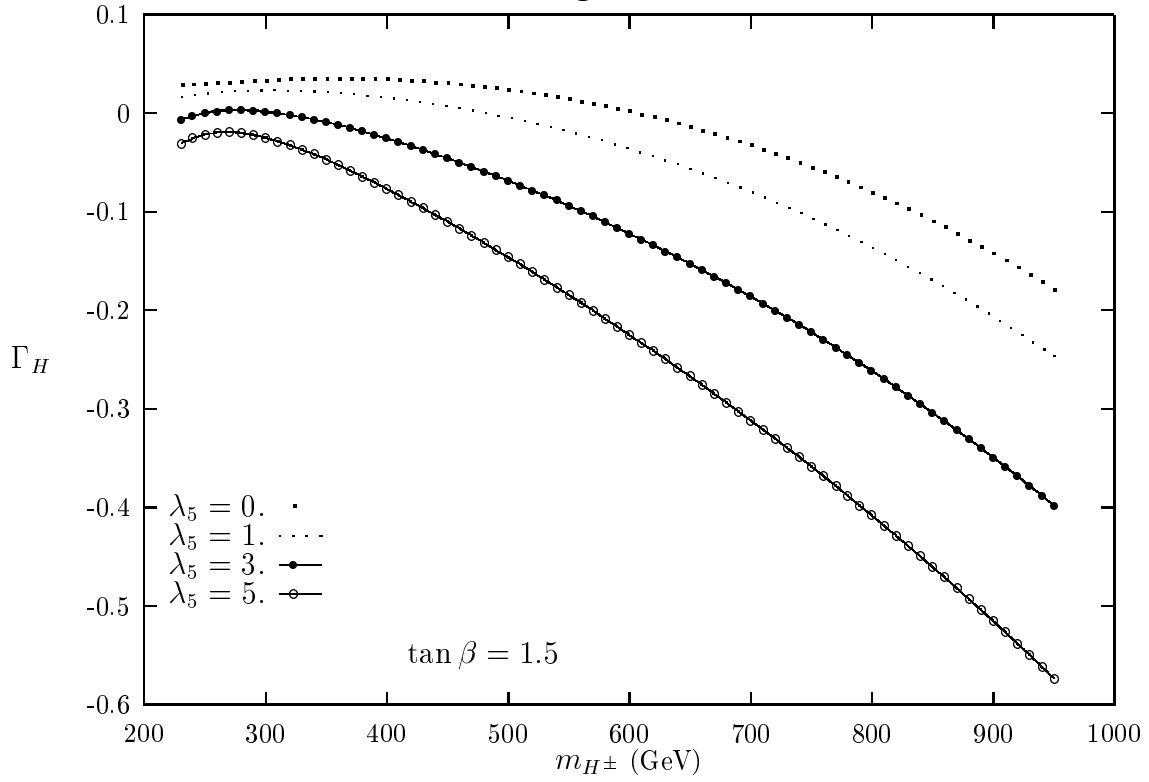


Figure. 3

Figure. 4. a

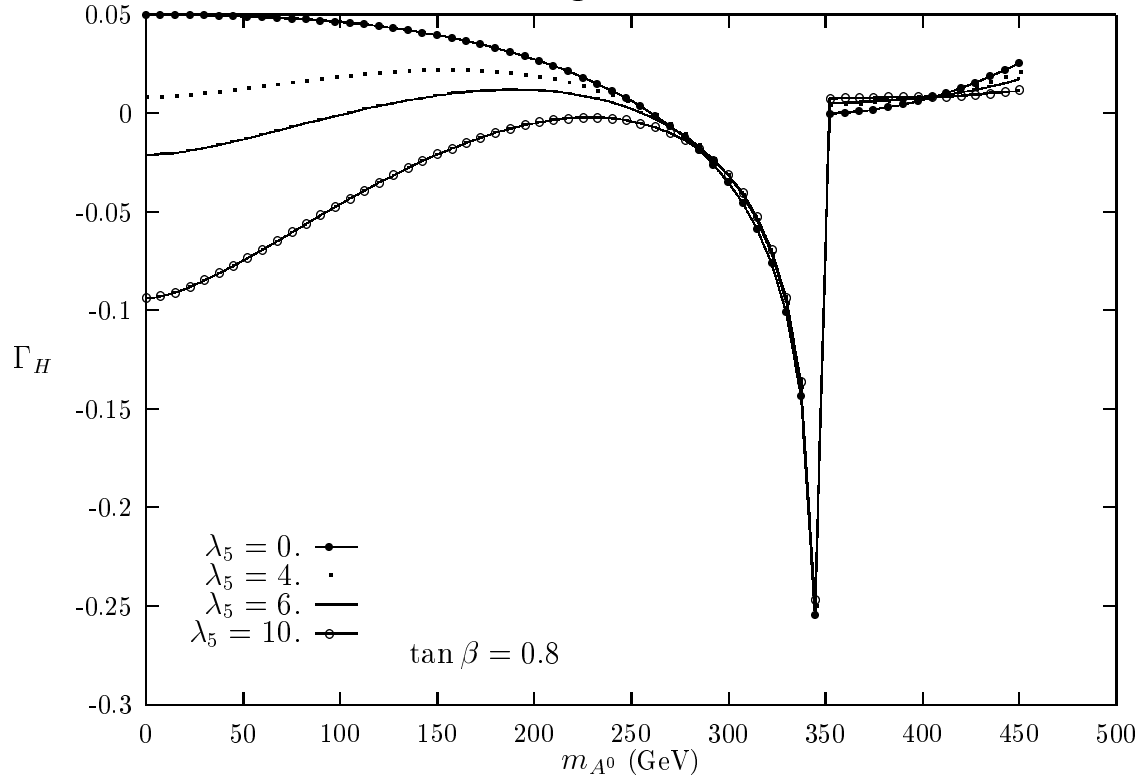


Figure. 4. b

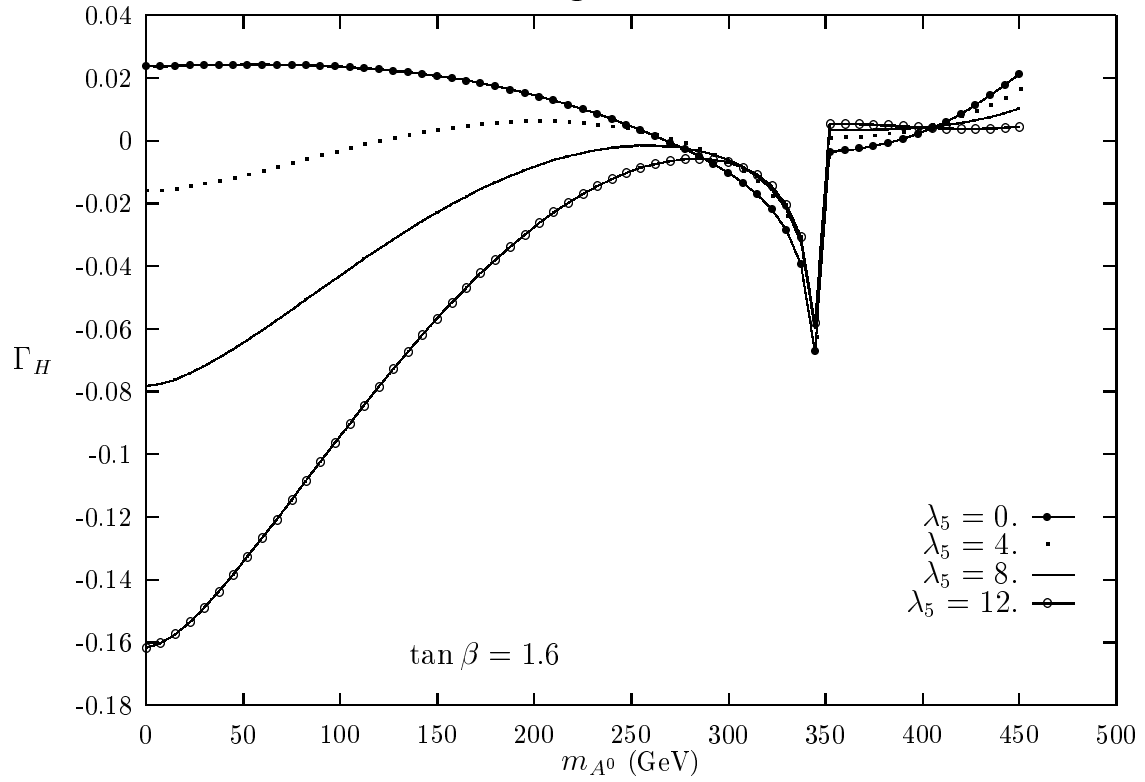


Figure. 4

Figure. 5

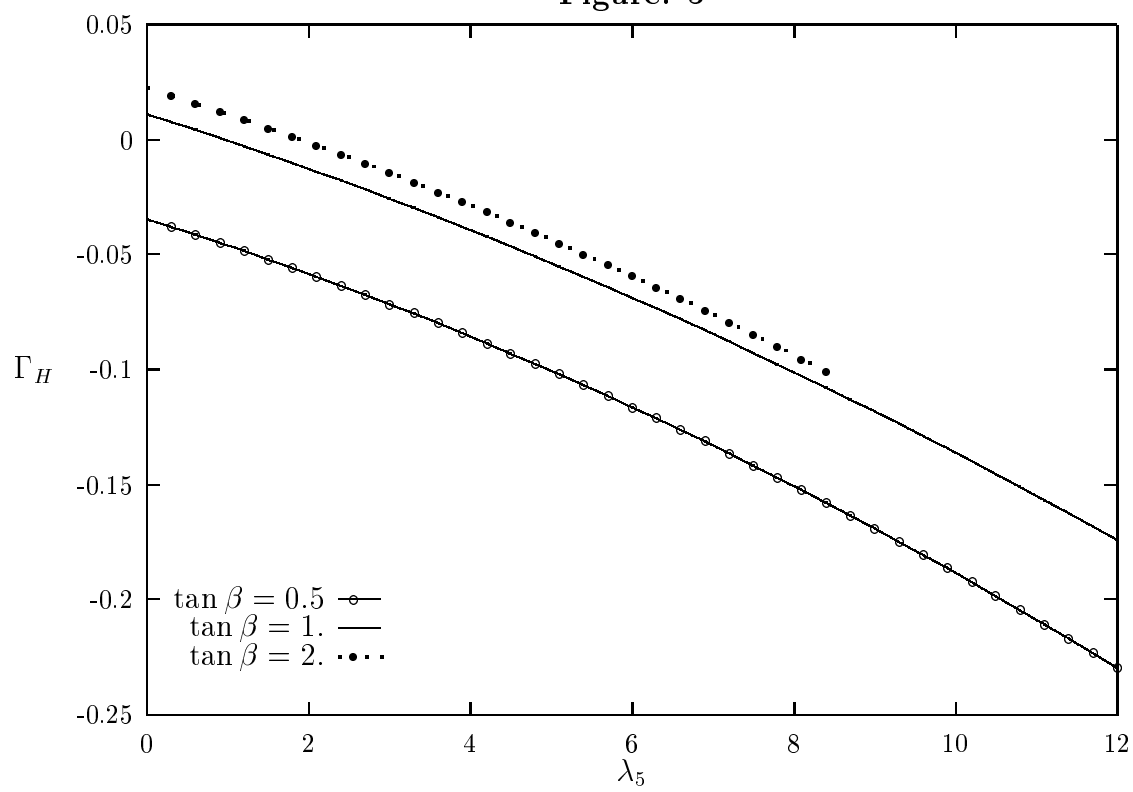


Figure. 5

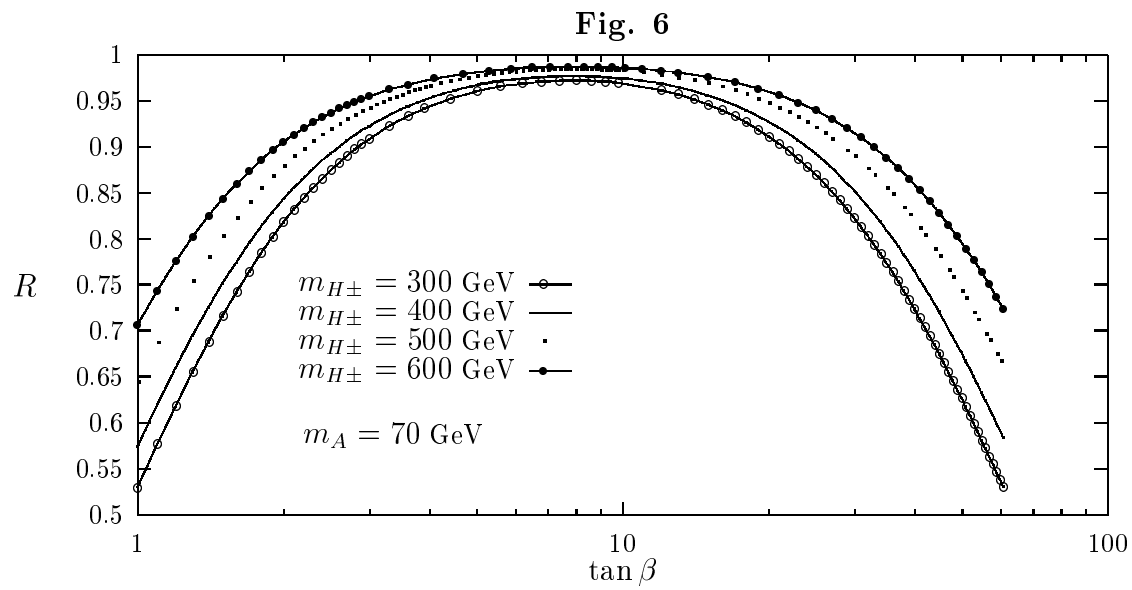


Figure. 6